Targeting EP2 receptor with multifaceted mechanisms for high-risk neuroblastoma

Ruida Hou[1], **Ying Yu**[1], **Madison N. Sluter**[1], **Lexiao Li**[1], **Jiukuan Hao**[2], **Jie Fang**[3], **Jun Yang**[3,4,5], **Jianxiong Jiang**[1,6,7,8,*]

[1]Department of Pharmaceutical Sciences, Drug Discovery Center, College of Pharmacy, University of Tennessee Health Science Center, Memphis, TN 38163, USA

[2]Department of Pharmacological and Pharmaceutical Sciences, College of Pharmacy, University of Houston, Houston, TX 77204, USA

[3]Department of Surgery, Comprehensive Cancer Center, St. Jude Children's Research Hospital, Memphis, TN 38105, USA

[4]Graduate School of Biomedical Sciences, St. Jude Children's Research Hospital, Memphis, TN 38105, USA

[5]Department of Pathology and Laboratory Medicine, College of Medicine, University of Tennessee Health Science Center, Memphis, TN 38163, USA

[6]Department of Anatomy and Neurobiology, College of Medicine, University of Tennessee Health Science Center, Memphis, TN 38163, USA

[7]Neuroscience Institute, University of Tennessee Health Science Center, Memphis, TN 38163, USA

[8]Lead contact

SUMMARY

Prostaglandin E_2 (PGE_2) promotes tumor cell proliferation, migration, and invasion, fostering an inflammation-enriched microenvironment that facilitates angiogenesis and immune evasion. However, the PGE_2 receptor subtype (EP1–EP4) involved in neuroblastoma (NB) growth remains elusive. Herein, we show that the EP2 receptor highly correlates with NB aggressiveness and acts as a predominant $G\alpha_s$-coupled receptor mediating PGE_2-initiated cyclic AMP (cAMP) signaling in NB cells with high-risk factors, including 11q deletion and *MYCN* amplification. Knockout of EP2 in NB cells blocks the development of xenografts, and its conditional knockdown prevents established tumors from progressing. Pharmacological inhibition of EP2 by our recently developed

*Correspondence: jjiang18@uthsc.edu.

antagonist TG6-129 suppresses the growth of NB xenografts in nude mice and syngeneic allografts in immunocompetent hosts, accompanied by anti-inflammatory, antiangiogenic, and apoptotic effects. This proof-of-concept study suggests that the PGE_2/EP2 signaling pathway contributes to NB malignancy and that EP2 inhibition by our drug-like compounds provides a promising strategy to treat this deadly pediatric cancer.

Graphical Abstract
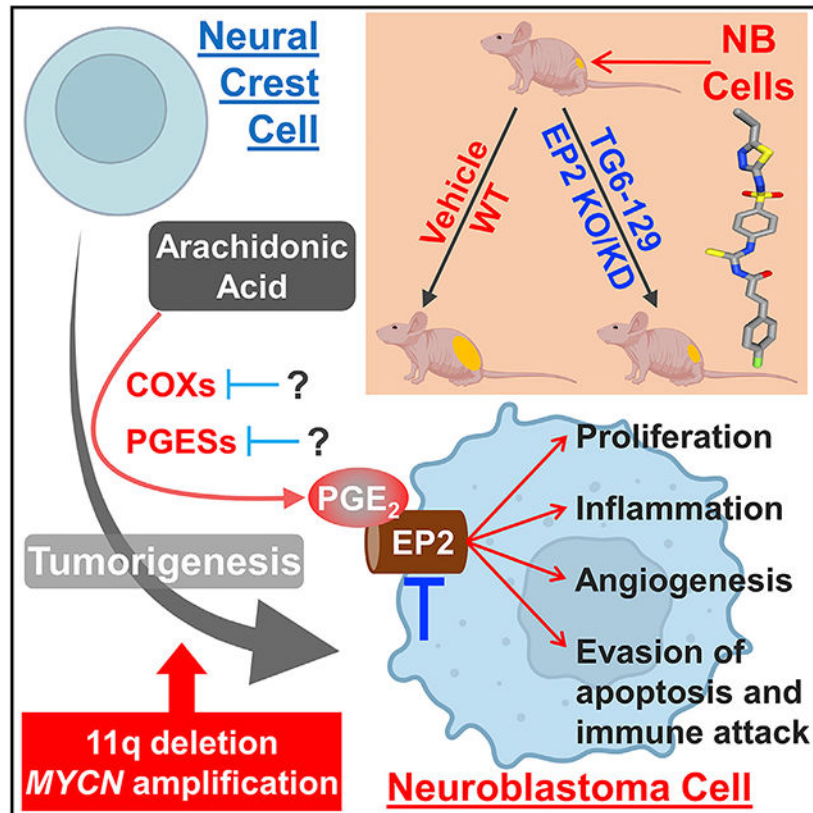
In brief

Hou et al. discover that prostaglandin receptor EP2 highly correlates with the aggressiveness of neuroblastoma, where it acts as the primary PGE_2 receptor mediating cAMP signaling. EP2 deficiency or inhibition suppresses neuroblastoma with high-risk factors including 11q deletion and *MYCN* amplification, demonstrating EP2 as a promising therapeutic target for neuroblastoma.

INTRODUCTION

Neuroblastoma (NB) is the most common extracranial solid tumor in childhood and accounts for ~7–10% of all pediatric cancers, causing ~15% of all cancer-related deaths in young children. Owing to the tremendous progress in tumor diagnosis and management, the survival of children with NB has much improved during the past decade. However, patients with high-risk NB still have a poor prognosis, because the 5-year survival rate remains below 50% even with intensive treatments: surgical resection along with chemotherapy,

radiotherapy, stem cell transplantation, and immunotherapy (Maris, 2010; Matthay et al., 2016). High risk, poor prognosis, and therapy resistance in NB are commonly associated with amplification of the transcription factor, N-Myc proto-oncogene (*MYCN*), deletion of chromosome 1p or 11q (Caren et al., 2010; Mlakar et al., 2017), gain-of-function mutations in the anaplastic lymphoma kinase (*ALK*) gene (George et al., 2008; Mosse et al., 2008; Trigg and Turner, 2018), and loss-of-function mutations in tumor suppressor p53 (*TP53*) (Imamura et al., 1993; Tweddle et al., 2003; Van Maerken et al., 2011). Among these, *MYCN* amplification is often associated with high-risk and poor-prognosis NB in younger children with an average age at diagnosis of less than 2 years, whereas the 11q deletion correlates with aggressive NB diagnosed in older children (~4 years), advanced disease stage, drug resistance, and decreased survival probability (Caren et al., 2010; Mlakar et al., 2017). Identifying new druggable targets and developing novel therapies for patients suffering from NB, particularly those who are in high-risk categories and developed resistance to current treatment, is in urgent demand.

As an essential component of the innate immune system, inflammation in the acute phase represents a protective strategy of the body to counteract injurious stimuli and to initiate the healing process. However, prolonged inflammation is also often associated with the occurrence and progression of a variety of tumors, including those of blood, brain, breast, colon, lung, pancreas, prostate, and skin (Grivennikov et al., 2010; Mantovani et al., 2008; Qiu et al., 2017). As such, cyclooxygenase (COX), a conventional inflammatory executor, has recently been demonstrated to provide an important driving force for NB pathogenesis (Carlson and Kogner, 2013). Oral intake of COX inhibitors, such as aspirin or diclofenac, can decrease the burden of tumors with *MYCN* amplification, reduce the presence of tumor-associated innate immune cells (Carlson et al., 2013), and delay the rapid progression of 11q-deleted NB (Larsson et al., 2015). COXs, with two isoforms COX-1 and COX-2, are the rate-limiting enzymes in the synthesis of bioactive lipids such as prostaglandin E_2 (PGE_2), which is highly present in tumor tissues and can increase tumor aggressiveness (Wang and Dubois, 2010). To synthesize PGE_2, arachidonic acid first is converted by COX to prostaglandin H_2 (PGH_2). Short-lived PGH_2 then is quickly catalyzed to PGE_2 by tissue-specific isomerases: prostaglandin E synthases (PGESs) comprising microsomal PGES-1 (mPGES-1), mPGES-2, and cytosolic PGES (cPGES) (Hirata and Narumiya, 2011). Among the three PGES isozymes, mPGES-1 is considered inducible and functionally coupled to COX-2 (Li et al., 2022; Samuelsson et al., 2007). Inhibition of mPGES-1 suppresses 11q-deleted NB (Kock et al., 2018), attesting to an essential role for PGE_2-mediated pro-inflammatory signaling in the development and progression of high-risk NB.

PGE_2 was demonstrated to regulate tumorigenesis through four G-protein-coupled receptors (GPCRs), EP1, EP2, EP3, and EP4, all of which were detected in human NB cells and tissues (Kock et al., 2018; Rasmuson et al., 2012). EP1 receptor is $G\alpha_q$ coupled to mediate the mobilization of cytosolic Ca^{2+} and activation of protein kinase C; both EP2 and EP4 are linked to $G\alpha_s$ activating adenylyl cyclase to generate cyclic AMP (cAMP); and EP3 is mainly coupled to $G\alpha_i$, and its activation downregulates cAMP signaling (Jiang et al., 2017). To date, the EP subtype underlying the COX/PGES/PGE_2 axis-driven tumor growth in NB remains elusive. Taking advantage of several bioavailable small-molecule compounds that we recently developed to suppress PGE_2-involved inflammation, we identified the

EP receptor subtype that contributes to the pathogenesis of NB. We also determined the therapeutic effects of a drug-like EP2 antagonist in mouse models of high-risk NB and explored the potential underlying mechanisms of action.

RESULTS

EP2 receptor is highly upregulated in human high-risk NB

To study the PGE_2 signaling in NB, we first examined the gene expression data in human NB samples from the R2 database. We analyzed the expression of the nine genes that are responsible for PGE_2 biosynthesis and signaling, including COX-1 (encoded by *PTGS1*), COX-2 (*PTGS2*), mPGES-1 (*PTGES*), mPGES-2 (*PTGES2*), cPGES (*PTGES3*), EP1 (*PTGER1*), EP2 (*PTGER2*), EP3 (*PTGER3*), and EP4 (*PTGER4*) in the SEQC cohort (N = 498), a large NB RNA sequencing (RNA-seq) dataset. We found that, among these nine genes, the expression of EP2 showed the highest increase in tumors of nonsurvival patients when compared with survival patients. In contrast, the expression of EP3 and EP4 was significantly decreased in the nonsurvival group (Figure 1A). Kaplan-Meier survival analyses on the SEQC cohort show that overall, more than 70% of patients with high EP2-expressing tumors deceased in 4 years; nearly 70% of patients with low EP2-expressing tumors eventually survived (Figure 1B). This significant relationship between high EP2 expression and poor overall survival was also unanimously found in the other three major patient cohorts of the R2 database: Kocak, Versteeg, and NRC (p < 0.0001; Figure 1B). To avoid any potential selection bias that might be introduced by the software, we reanalyzed these cohorts with equal or similar patient numbers in each group and found the same outcomes in datasets Kocak, Versteeg, and NRC (p < 0.01; Figure S1). The SEQC cohort showed a similar trend, although it was not statistically significant (Figure S1).

Amplification of the MYC family member, *MYCN,* has been found in ~25% of NB cases and highly correlates with the high-risk disease and poor prognosis, particularly in infants (Irwin et al., 2021). Currently, *MYCN* amplification is still the best-characterized genetic marker of high risk and chemoresistance in NB (Huang and Weiss, 2013). Notably, the EP2 receptor is expressed substantially higher in NB with *MYCN* amplification than those with normal status of *MYCN* across all four major NB cohorts (Figure 1C), suggesting a strong positive relationship between PGE_2/EP2 signaling and the most common risk factor in NB. On the contrary, the other three EP subtypes (EP1, EP3, and EP4) consistently showed an inverse correlation with *MYCN* in NB (Figure S2).

EP2 receptor activation can upregulate a variety of tumor-promoting cytokines, chemokines, growth factors, and their responding receptors, thereby amplifying tumor-related inflammation, nurturing the tumor microenvironment, and promoting growth of tumors in prostate, skin, colon, and brain (Jiang and Dingledine, 2013b; Khan et al., 2022; Ma et al., 2015; Merz et al., 2016; Qiu et al., 2019; Sung et al., 2005). We next examined the expression of a variety of common pro-tumor mediators in NB that may regulate tumor cell survival, invasion, migration, proliferation, angiogenesis, and immune escape. Pearson's correlation coefficient analyses revealed significant positive correlations of expression between EP2 and a large proportion of these cytokines, chemokines, growth factors, and receptors (40/45, ~89%) in at least two of the four major R2 NB datasets: SEQC, Kocak,

Versteeg, and NRC (Figure 1D). These potential NB facilitators include ALK (Trigg and Turner, 2018), brain-derived neurotrophic factor (BDNF) (Middlemas et al., 1999), chemokine (C-C motif) ligand 2 (CCL2) or monocyte chemoattractant protein 1 (MCP-1)/C-C chemokine receptor type 2 (CCR2) (Metelitsa et al., 2004), colony-stimulating factor 1 (CSF-1)/CSF-1 receptor (CSF1R) (Webb et al., 2018), chemokine (C-X3-C motif) ligand 1 (CX3CL1)/CX3CR1 (Nevo et al., 2009), CXCL2/CXCR2 (Hashimoto et al., 2016), CXCL12/CXCR4/CXCR7 (Liberman et al., 2012), epidermal growth factor receptor (EGFR) (Ho et al., 2005), endoglin (ENG) or cluster of differentiation 105 (CD105) (Cavar et al., 2015; Pezzolo et al., 2007; Wu et al., 2019), glial cell line-derived neurotrophic factor (GDNF)/GDNF family receptor $\alpha1$ (GFRA1) (Hansford and Marshall, 2005; Hishiki et al., 1998), insulin-like growth factor 2 (IGF2)/IGF2 receptor (IGF2R) (El-Badry et al., 1991; Mohlin et al., 2013), interleukin (IL)-1β/IL-1R (Elaraj et al., 2006), IL-6/IL-6R (Ara et al., 2013; Pistoia et al., 2011), macrophage inhibitory cytokine 1 (MIC-1) (Craig et al., 2016), matrix metallopeptidases (MMPs) (Nyalendo et al., 2009; Sugiura et al., 1998), nuclear factor κB (NF-κB) (Spel et al., 2018; Zhi et al., 2014, 2015), platelet-derived growth factor receptor β (PDGFRB) (Kock et al., 2018), platelet endothelial cell adhesion molecule 1 (PECAM-1) or CD31 (Pezzolo et al., 2007), periostin (POSTN) (Sasaki et al., 2002), retinoic acid receptor responder protein 2 (RARRES2)/chemokine-like receptor 1 (CMKLR1) (Tummler et al., 2017), signal transducer and activator of transcription 3 (STAT3) (Hadjidaniel et al., 2017), transforming growth factor $\beta1$ (TGF-$\beta1$) (Castriconi et al., 2013), vascular endothelial growth factor (VEGF)/VEGF receptor (VEGFR) (Becker et al., 2010; Jakovljevic et al., 2009; Weng et al., 2017), as well as the VGF nerve growth factor inducible (Rossi et al., 1992) (Tables S1-S4). These consistent findings from analyzing the NB patient datasets reveal that the elevated EP2 expression is highly associated with the increased malignancy of NB tumors, leading us to hypothesize that PGE$_2$ signaling via the EP2 receptor might contribute to COX activity-mediated NB growth.

PGE$_2$ mediates Gα_s-dependent signaling via EP2 in NB cells

The expression of PGE$_2$ signaling-associated genes, including COXs, PGESs, and EPs, was previously demonstrated in human NB cells and tissues (Kock et al., 2018; Rasmuson et al., 2012); however, gene expression does not necessarily correlate with signaling activity. To validate PGE$_2$/EP pathways in NB, we next investigated the PGE$_2$-mediated cAMP signaling in human NB cell lines with various risk factors, such as 11q deletion (SK-N-AS), gain-of-function mutation of ALK (SK-N-SH and SH-SY5Y), P53 dysfunction (CHLA-90), KRAS mutation (NB-EBc1), and *MYCN* amplification (SK-N-BE(2), BE(2)-C, CHLA-136, SiMa, IMR-32, and NB-1691), as well as mouse NB cell lines Neuro-2a and NXS2. We treated these cells with a relatively high concentration (10 μM) of PGE$_2$, selective EP2 receptor agonist butaprost, or EP4 agonist CAY10598, aiming to fully activate their EP2 and EP4 receptors. The human fibroblast cell line Hs68 was also included in the experiment as normal control cells (Yang et al., 2017). About 40 min after the stimulation began, cAMP levels in these cells were measured by a time-resolved fluorescence energy transfer (TR-FRET) assay, in which a reduction of FRET signal indicates an increase in cAMP. We found that PGE$_2$ and butaprost, but not CAY10598, induced cAMP accumulation in all examined human and mouse NB cell lines to a degree similar to that of forskolin (Figure 2A), a direct activator of the adenylyl cyclase commonly used to indicate the maximal capability of the

cells to generate cAMP. In contrast, stimulation with EP4 agonist CAY10598 led to more cAMP production than EP2 agonist butaprost and PGE_2 in the normal human fibroblast cell line Hs68 (Figure 2A). It appears that EP2, compared with the much less active EP4, is the dominant $G\alpha_s$-coupled receptor that mediates PGE_2-initaited cAMP signaling across all these tested NB cells with various high-risk factors (p < 0.0001; Figure 2B). These findings confirm that EP2 expression is ubiquitously elevated in high-risk NB cells, leading to its dominant role transducing the PGE_2-mediated cAMP signaling in these tumor cells.

We next focused on the NB cell line SK-N-AS, which has high *c-MYC* expression and possesses a high-risk factor: 11q deletion (O'Brien et al., 2016; Zimmerman et al., 2018). Our TR-FRET assay on SK-N-AS cells revealed that PGE_2 and butaprost, but not CAY10598, activated EP2 receptor in a concentration-dependent manner and 1 μM agonist (PGE_2 or butaprost) nearly maximized the cell response, evidenced by the plateau of concentration-response curves when higher concentrations were applied (Figure 3A). We previously reported a series of EP2-selective small-molecule antagonists (Figure 3B), such as TG4-155 (Jiang et al., 2012), TG6-10-1 (Jiang et al., 2013), TG6-129 (SID17503974) and SID26671393 (Ganesh et al., 2013), which together with Pfizer compound PF04418948 are among the first-generation EP2 antagonists with high potency and selectivity (Sluter et al., 2021). All our EP2 antagonists have drug-like properties with favorable ADME (absorption, distribution, metabolism, excretion) predicted by QikProp software (Schrödinger) (Table S5). Here, these compounds were tested for the inhibition on EP2 in SK-N-AS cells, which were stimulated with 1 μM PGE_2 to maximize the cytosol cAMP. It appears that all these EP2 antagonists were able to robustly decrease PGE_2-induced cAMP signaling in SK-N-AS cells in a concentration-dependent manner (Figure 3C). In contrast, GW627368X, an EP4-selective antagonist, had no effect on PGE_2-induced cAMP signaling in these cells, evidenced by a completely flat concentration-response curve (Figure 3C).

By comparison at the same concentration (1 μM), TG4-155 showed the highest potency of EP2 antagonism in NB cells, followed by TG6-129, PF-04418948, TG6-10-1, and SID26671393 in order, demonstrated by the rightward shift of their PGE_2 concentration-response curves compared with the control (Figure 3D). Conversely, at the same test concentration (1 μM), EP4 antagonist GW627368X failed to shift the PGE_2 response curve in SK-N-AS cells (Figure 3D), confirming the lack of functioning EP4 receptor in these human NB cells. The TR-FRET assay further suggested that the tested compounds inhibited PGE_2-induced human EP2 activation in SK-N-AS cells in a concentration-dependent manner, exemplified by TG6-129 and SID26671393 (Figure 3E). Schild regression analyses revealed that our compounds TG4-155, TG6-129, TG6-10-1, and SID26671393 inhibited the EP2 receptor via a competitive mechanism, and their K_B values for EP2 receptor in SK-N-AS cells were 2.25, 5.96, 10.5, and 30.3 nM, respectively (Figure 3F). These TR-FRET results together identified a robust PGE_2/EP2/cAMP signaling that ubiquitously exists in various human NB cells and can be highly effectively blocked by our selective EP2 antagonists.

PGE$_2$/EP2 signaling in NB cells is required for tumorigenesis

The dominant role for EP2 receptor in PGE$_2$-initiated cAMP signaling in NB cells motivated us to test the hypothesis that EP2 activation might contribute to the proliferation of NB. We began with the SK-N-AS cell line because it is a 11q-deleted NB cell line showing aggressive proliferation *in vivo* and has been widely used in xenograft models (Kock et al., 2018; Larsson et al., 2015). We first generated SK-N-AS cell lines lacking the EP2 utilizing CRISPR-Cas9-based genome editing with two single guide RNAs (sgRNAs) targeting different regions of the EP2 gene. EP2 ablation was confirmed by qPCR that detected mRNA expression of EP2 in the wild-type (WT) cell line, but not in the two knockout (KO) cell lines (KO1 and KO2) (Figure 4A). The effectiveness of EP2 deletion was further validated by the lack of cAMP response to PGE$_2$ in the two KO cell lines when compared with the WT cell line, detected by the cell-based TR-FRET assay (Figure 4B). We next examined the effects of EP2 ablation on tumorigenic activities of SK-N-AS cells and found that the neurospheres formed by the two EP2-deficient cell lines on average were substantially smaller than those derived from the WT cells (Figure 4C). Likewise, EP2 deletion also considerably decreased the density of colonies developed by the SK-N-AS cells (Figure 4D). Moreover, treatment with EP2 antagonist TG6-129 reduced both neurosphere size and colony density of the WT NB cell line but had no effect on the two EP2-deleted cell lines (Figures 4C and 4D). The lack of effect of TG6-129 on two NB cell lines without EP2 expression validated the PGE$_2$ receptor as the molecular target of our compound in NB cells.

We then determined the consequences of the genetic deletion of the EP2 receptor in the development of NB *in vivo*. WT or EP2 KO SK-N-AS cells were inoculated into athymic nude mice to generate high-risk tumors with 11q deletion. After solid tumors became visible and assessable, tumor volumes were measured daily for comparisons of WT and KO groups. Tumors generated by EP2-ablated NB cells showed a significant decrease in volumes when compared with the WT NB ($p < 0.001$ at measurement days 20–23), whereas there was no difference in tumor volume between the two KO groups (Figure 4E). Intriguingly, the growth of tumors formed by the two EP2 KO cell lines appeared to be completely prevented, demonstrated by the virtually flat tumor growth curves (Figure 4E). The WT tumors were physically larger than those formed by EP2 KO cells, whereas the tumors formed by the two EP2 KO cell lines did not differ from each other (Figure 4F). Notably, the average weight of EP2 KO tumors was only about less than 10% of the tumors generated by the WT NB cells ($p = 0.012$; Figure 4G). The lack of EP2 expression in tumors formed by these two EP2-deficient NB cell lines was confirmed by immunohistochemistry (Figure 4H). Other than the tumor burden, mice were overall healthy without showing any behavioral abnormality or weight loss. Taken together, these findings suggest that the EP2 activity is required for the human high-risk NB cells to develop tumors.

Conditional knockdown or pharmacological inhibition of EP2 impairs NB

The blockade of tumor formation by EP2 ablation in NB cells inspired us to study the effects of inducible short hairpin RNA (shRNA)-mediated knockdown (KD) of the receptor in established tumors. We first created SK-N-AS cells in which EP2 expression was reduced to only about one-third of that in WT cells after treatment with doxycycline to induce EP2

shRNA (Figure 5A). We then inoculated the WT and EP2 KD cells into athymic nude mice to create xenografts. With solid tumors visibly developed, mice were treated with doxycycline daily to downregulate EP2. We found that the doxycycline-induced KD of EP2 substantially decreased tumor volumes when compared with the WT control ($p < 0.001$ at measurement days 20–26; Figure 5B). After dissection of tumors for analyses (Figure 5C), it was found that the tumor weights on average were considerably reduced by EP2 KD ($p = 0.0004$; Figure 5D). The doxycycline-induced reduction in EP2 expression of KD tumors was confirmed by immunohistochemistry (Figure 5E). These results suggest that the conditional inducible KD of EP2 in NB cells after tumors were established was able to suppress their further development and progression.

The encouraging results from studies on CRISPR-Cas9-based KO and inducible shRNA-mediated conditional KD of EP2 led us to determine the effects of pharmacological inhibition of EP2 by our antagonists in NB cells on the development and progression of tumors. We chose to test compound TG6-129 for EP2 receptor inhibition in NB models because it has a longer terminal half-life (2.7 h) in mice than compounds TG4-155 (0.6 h) and TG6-101 (1.6 h) (Figure 3G) (Du et al., 2016; Ganesh et al., 2013; Jiang et al., 2012). To test TG6-129 in NB xenografts, each mouse was inoculated with SK-N-AS cells into two different flank sites. After solid tumors were developed, animals were randomized and treated with TG6-129 (0, 10, or 20 mg/kg intraperitoneally [i.p.]). The mice were treated only once daily because, with a single systemic injection (10 mg/kg i.p.) in mice, the projected concentration of TG6-129 in the circulatory system should be above its EP2 IC_{50} value (192 ng/mL or 0.39 μM; Figure 3C) in NB cells for up to 24 h (Figure 3G). The tumor volumes were measured on a daily basis and compared between treatment groups. After treatment for 18 days, tumors were collected, weighed, and analyzed. Interestingly, TG6-129-treated mice (both 10 and 20 mg/kg) showed significant decreases in tumor size when compared with vehicle-treated mice ($p < 0.001$ at days 15–18; Figure 5F). The weight of SK-N-AS tumors on average was decreased to ~35–40% of control by treatment with TG6-129 ($p = 0.003$ and 0.005 for 10 and 20 mg/kg, respectively; Figure 5G). Other than the tumor burden, animals from all groups were overall healthy without showing any behavioral abnormality or considerable weight loss by the treatment with vehicle or TG6-129. Our data together suggest that PGE_2 cAMP signaling via EP2 is involved in NB growth, and this $G\alpha_s$-coupled receptor might represent a potential molecular target for NB treatment.

We next performed immunohistochemistry to examine the effects of EP2 inhibition by TG6-129 on the proliferative index of NB cells *in vivo*. Immunostaining for Ki-67, a nuclear protein commonly used as a cellular marker for proliferation, was utilized to identify proliferating cells in subcutaneous NB tissues. We found that the systemic treatment with TG6-129 substantially decreased the proliferation of tumors formed by SK-N-AS cells in a dose-dependent manner: 25% reduction by 10 mg/kg dose and 55% reduction by 20 mg/kg dose ($p = 0.004$ and $p < 0.001$ for 10 and 20 mg/kg, respectively; Figure 5H). These findings indicate that the PGE_2 signaling via EP2 receptor promotes the tumorigenic potential of high-risk NB cells.

Microvascular proliferation is a hallmark of higher malignancy and a cardinal characteristic of NB, especially in the advanced and aggressive stages (Rossler et al., 2008). It is

often indicated by the expression of the PECAM-1 or CD31, a common biomarker for angiogenesis in various tumors (DeLisser et al., 1997). We were thereby interested in determining whether PGE_2 signaling via EP2 receptor contributes to the elevation of CD31 in NB. We first performed CD31 immunofluorescent staining of 11q-deleted xenograft samples and quantitated their vascular areas. We found that TG6-129 treatment largely decreased the vascular areas in SK-N-AS cell-derived tumors in a dose-dependent manner: 63% reduction by 10 mg/kg TG6-129 and 87% reduction by 20 mg/kg dose (p = 0.025 and p = 0.004, respectively; Figure 5I). We next examined the expression of CD31 in NB from the four major human patient cohort studies on R2 database platform (SEQC, Kocak, Versteeg, and NRC) and found that the EP2 receptor consistently displayed positive correlation in expression with CD31 across all these patient datasets (Figure S3). Similar outcomes were found between EP2 and several other common angiogenesis biomarkers important for NB, such as VEGF and VEGFR (Figure 1D) (Jakovljevic et al., 2009), as well as ENG (also known as CD105, encoded by *ENG*) (Figure S4), which contributes to the tumor microenvironment and treatment resistance in NB (Cavar et al., 2015; Pezzolo et al., 2007; Wu et al., 2019). These findings, taken together, revealed an essential role for PGE_2 signaling via EP2 in microvascular proliferation of high-risk NB.

Pharmacological inhibition of EP2 suppresses *MYCN*-amplified NB

The amplification of proto-oncogene *MYCN* is the most common and best-characterized genetic marker of high risk in NB to date (Huang and Weiss, 2013; Irwin et al., 2021); therefore, we next investigated the role of EP2 receptor in *MYCN*-amplified NB. We first examined the PGE_2-mediated cAMP signaling in human NB cell line BE(2)-C, in which *MYCN* is highly amplified and expressed. Treatment with PGE_2 and selective EP2 agonist butaprost, but not the selective EP4 agonist CAY10598, induced concentration-dependent cAMP synthesis in BE(2)-C cells (Figure 6A). We further found that the PGE_2-stimulated cAMP signaling in these cells was inhibited by EP2 antagonist TG6-129 also in a concentration-dependent manner (Figure 6B), suggesting that the EP2 is a dominant $G\alpha_s$-coupled receptor in BE(2)-C cell line. It appeared that our compound TG6-129 inhibited EP2 receptor activation in BE(2)-C cells via a competitive mechanism with a Schild K_B of 7.72 nM (Figure 6C), which is very similar to that in 11q-deleted SK-N-AS cells (5.96 nM; Figure 3F), demonstrating the effectiveness of our EP2 antagonists in blocking the PGE_2/EP2 signaling in NB cells with distinct risk factors.

We then evaluated the effects of pharmacological inhibition of the EP2 receptor on *MYCN*-amplified tumors formed by BE(2)-C cells in athymic nude mice. After solid tumors were developed, mice were treated by vehicle or EP2 antagonist TG6-129 (20 mg/kg i.p.) for about 3 weeks, followed by dissection of tumors for comparisons. TG6-129-treated mice showed a significant decrease in tumor volumes when compared with vehicle-treated mice (p < 0.001 at days 17–21; Figure 6D). The weight of *MYCN*-amplified tumors on average was reduced to nearly 60% with treatment of TG6-129, when compared with vehicle treatment (p = 0.0376; Figure 6E). Other than the tumor burden, mice were overall healthy and did not display any behavioral deficits or considerable weight loss.

Among the five types of prostanoid, PGE_2 is most relevant to tumorigenesis and is well known for its multifaceted roles in tumor-associated inflammation and microenvironment (Nakanishi and Rosenberg, 2013; Wang and DuBois, 2016). PGE_2 receptor EP2 is highly correlated to several key pro-inflammatory cytokines in NB, such as IL-1β and IL-6 ($p < 0.001$; Figure 1D). We then performed immunostaining for IL-1β and IL-6 to indicate the inflammation in subcutaneous tumors and found that both cytokine levels were substantially diminished in BE(2)-C tumors from EP2 antagonist-treated mice compared with their vehicle-treated peers ($p = 0.003$ for IL-1β; $p = 0.0057$ for IL-6; Figure 6F). Immunostaining results further revealed that levels of apoptotic markers cleaved caspase-3 (c-Casp3) and poly (ADP-ribose) polymerase (c-PARP) were increased in TG6-129-treated xenografts ($p < 0.001$; Figure 6G), indicating that an apoptotic mechanism might be involved in suppressive effects of EP2 antagonism on *MYCN*-amplified NB.

EP2 inhibition suppresses syngeneic NB in immunocompetent hosts

PGE_2 has long been known as an essential immune modulator and plays considerable roles in regulating the inflammatory microenvironments (Aoki and Narumiya, 2017; Ma et al., 2015). We next evaluated the effects of TG6-129 on syngeneic tumors formed by mouse NB cell line NXS2 in A/J inbred mice. Resembling human NB cell lines, NXS2 also engages EP2 as a predominant $G\alpha_s$-coupled PGE_2 receptor to mediate cAMP signaling (Figure 2A). The NXS2 cell line was originally derived from A/J mice and expresses *MYCN* (Lode et al., 1997; Stermann et al., 2015). The identical strain of host and cell line prevents tumor rejection, allowing testing of immune/inflammation-targeting agents in immunocompetent hosts. After solid syngeneic tumors were developed, A/J mice were treated by vehicle or EP2 antagonist TG6-129 (20 mg/kg i.p.) for about 3 weeks, followed by dissection of tumors for analyses and comparisons. It appeared that TG6-129-treated mice showed a significant decrease in tumor volumes when compared with vehicle-treated mice ($p < 0.001$ at days 17–20; Figure 7A). The weight of allografts on average was reduced to ~63% by treatment with TG6-129 ($p = 0.0329$; Figure 7B). Other than the tumor burden, mice in general were healthy and did not show noticeable behavioral abnormality or significant weight loss.

Immunostaining results further revealed that the treatment with our EP2 antagonist TG6-129 decreased the tumor cell proliferation indicated by Ki-67 expression and the microvascular areas illustrated by CD31/PECAM1 distribution in tumor tissues ($p = 0.0002$ for Ki-67; $p = 0.0022$ for CD31; Figure 7C). Likewise, the expression of pro-inflammatory cytokines IL-1β and IL-6 was also substantially reduced in tumors of mice that were treated by the EP2 antagonist when compared with vehicle control ($p = 0.0008$ for IL-1β; $p < 0.0001$ for IL-6; Figure 7D). In line with results in xenografts, the levels of both apoptotic markers c-Casp3 and c-PARP were increased in TG6-129-treated allografts ($p = 0.0099$ for c-Casp3; $p = 0.0005$ for c-PARP; Figure 7E). These findings collectively suggest that the suppressive effects of EP2 inhibition on syngeneic allografts are positively associated with reductions in tumor cell proliferation, angiogenesis, and inflammatory cytokines. Given that the tumor growth was not fully inhibited and there was no indication of tumor shrinkage in TG6-129-treated animals, whether apoptotic mechanisms are involved in TG6-129-mediated tumor suppression remains to be determined.

DISCUSSION

We performed comprehensive analyses of gene expression and survival probability in several large cohort studies of NB patients, which led us to hypothesize that PGE_2 signaling via EP2 receptor plays an essential role in COX activity-associated NB growth. We tested this hypothesis using both pharmacological and genetic approaches and demonstrated that EP2 is the dominant $G\alpha s$-coupled receptor that mediates COX/PGES/PGE_2/cAMP signaling in NB cells with high-risk factors, such as *MYCN* amplification and 11q deletion. We showed that genetic ablation and conditional depletion of EP2 were able to impair the development and progression of NB xenografts, respectively. Our results also demonstrated that pharmacological inhibition of EP2 by a bioavailable small-molecule antagonist TG6-129 substantially decreased the aggressiveness of high-risk NB cells. Importantly, results from studies on xenografts in nude mice were largely recapitulated in syngeneic tumors developed in immunocompetent hosts. Lastly, EP2 inhibition by TG6-129 showed anti-inflammatory, antiangiogenic, and apoptotic effects in NB, which may underlie the mechanisms of its anti-proliferative actions. Taken together, our findings establish PGE_2 receptor EP2 as an appealing therapeutic target for high-risk NB.

COX activity is often elevated in tumor tissues, and its expression level is highly correlated with tumor aggressiveness (Mantovani et al., 2008; Wang and Dubois, 2010). COX thus was once considered as a favorable therapeutic target for various cancers. However, the feasibility of blocking COX cascade using nonsteroidal anti-inflammatory drugs (NSAIDs) or COX-2-selective inhibitors (Coxibs) to interrupt the tumor progression has been dampened. Long-term consumption of these drugs can increase the potential risk of adversative effects particularly on gastrointestinal tract and microvascular systems that may lead to myocardial infarction, stroke, and even mortality (Grosser et al., 2010). The past two decades already witnessed a mounting recognition of these life-threatening consequences and the subsequent withdrawal of two legendary COX-2 inhibitor drugs, rofecoxib and valdecoxib. These disappointing outcomes are not unanticipated, because COX activity leads to the synthesis of five types of prostanoids that in turn can activate a total of nine GPCRs, implementing a myriad of detrimental and beneficial actions (Hirata and Narumiya, 2011; O'Callaghan and Houston, 2015; Wang and Dubois, 2010). Particularly, COX inhibition can decrease the systemic prostacyclin (also known as prostaglandin I_2 [PGI_2]), another enzymatic product of COX that acts as a vasodilator and platelet inhibitor, thereby increasing cardiovascular risk (Yu et al., 2012). This monumental lesson, although disheartening, inspired us and others to seek the next-generation therapeutic targets from the COX downstream prostanoid synthases or receptors (Jiang and Dingledine, 2013a; Jiang et al., 2017). As such, blocking mPGES-1 enzyme has been proposed as an alternative strategy to suppress NB tumor growth, which is considered more specific than COX inhibition because it disrupts only PGE_2 synthesis without affecting other COX-derived biolipids like PGD_2, $PGF_{2\alpha}$, and PGI_2 (Kock et al., 2018, 2020). Likewise, in this work, we presented evidence that targeting PGE_2 receptor EP2 might represent another feasible therapeutic strategy for NB. Blocking EP2 activation potentially provides even higher therapeutic specificity than inhibiting mPGES-1 because it should not affect other PGE_2

receptor subtypes, particularly EP3 and EP4, whose expression in NB is correlated with the decreased aggressiveness (Figure 1A) and low N-Myc expression (Figure S2).

PGE_2 has been reported to regulate tumorigenesis through all four EP receptors, among which the $G\alpha_s$-coupled EP2 and EP4 have been mostly studied for their potential roles in the development and progression of tumors, including those of breast, colon, lung, ovary, prostate, skin, and stomach (Hsu et al., 2017; Jain et al., 2008; Jiang and Dingledine, 2013a; Ma et al., 2012; Okuyama et al., 2002; Rundhaug et al., 2011; Spinella et al., 2004; Wang et al., 2018). It appears that EP2 and EP4 are ubiquitously present in most tumors and likely function synergistically to enhance cancer cell activities because both receptors in a very similar way can trigger cAMP signaling, as well as the G protein-independent pathway (Jiang et al., 2017). However, in contrast with EP2 receptor's tumor-promoting roles in NB, the EP4 signaling appears to be positively associated with the probability of survival in NB patients (Figure 1A). Moreover, there is an inverse correlation of EP4 receptor and *MYCN* expression with similar results in R2 NB datasets (Figure S2). Indeed, the PGE_2-promoted cAMP singling in various human NB cell lines is mainly mediated by the EP2 receptor, although some of these cells might also express functional EP4 at relatively low levels (Figure 2A). Conversely, EP4 is the dominant PGE_2 receptor subtype for cAMP production in normal human fibroblast cells (Figure 2A). Nonetheless, whether the EP4 receptor signaling down- or upregulates the growth of NB remains to be determined.

PGE_2 signaling via EP2 receptor has emerged as an essential contributor to tumor growth engaging mechanisms including, but not limited to, (1) inducing reactive mediators for tumor cell growth, including pro-inflammatory cytokines and growth factors (Donnini et al., 2007; Jiang and Dingledine, 2013b; Ma et al., 2015; Merz et al., 2016); (2) promoting angiogenesis via activating VEGF and fibroblast growth factor (Finetti et al., 2008; Kamiyama et al., 2006; Trau et al., 2016); and (3) creating immunosuppressive microenvironments that allow tumor cells to escape immunosurveillance (Aoki and Narumiya, 2017; Khan et al., 2022; O'Brien et al., 2014). The molecular mechanisms by which PGE_2/EP2 signaling promotes NB progression are not fully understood. However, we previously revealed that EP2 receptor activation can induce pro-inflammatory cytokines (Jiang and Dingledine, 2013b; Jiang et al., 2012; Quan et al., 2013). Indeed, we showed here a positive correlation between EP2 and a flock of essential tumor-promoting cytokines, chemokines, growth factors, and corresponding receptors in human NB tumors (Tables S1-S4). Particularly, the expression of EP2 receptor is highly correlated with that of a number of the most pronounced angiogenesis biomarkers, including PECAM-1 (CD31) and ENG (CD105) (Figures 1D, S3, and S4), indicating an angiogenic role of PGE_2/EP2 signaling in NB. The likely involvement of EP2 receptor in microvascular proliferation of NB was further supported by evidence that EP2 inhibition by TG6-129 decreased the CD31 levels in high-risk NB xenografts and allografts (Figures 5I and 7C). However, our results cannot exclude the possibility that the downregulated CD31 in tumor tissues was merely a consequence of reduced NB cell proliferation, because smaller tumors likely require less vascularization to survive. In contrast with the well-known conception that angiogenesis is a major contributory factor in creating malignant NB (Roy Choudhury et al., 2012), some angiogenic growth factors and receptors, such as VEGFA and VEGFR2, correlate to a favorable prognosis in patients with NB (Becker et al., 2010; Weng et al., 2017).

Intriguingly, this aligns with the finding that the EP2 receptor poorly correlates with VEGFA and VEGFR2, because their correlations were found to be nonsignificant in three of the four major R2 NB datasets (Figure 1D). Nevertheless, whether and how EP2 contributes to NB growth via promoting angiogenesis remains to be determined.

In summary, this work provides proof-of-concept evidence that PGE_2 signaling via EP2 receptor might represent an appealing anti-inflammatory target for the treatment of NB with various high-risk factors. The pharmacological study was guided by pharmacokinetic and pharmacodynamic properties of our EP2 antagonists and validated by genetic strategies using CRISPR-Cas9-based KO and inducible shRNA-mediated conditional KD. These findings together raise a notion that EP2 antagonism is an alternative strategy to inhibiting PGE_2 synthesis for chemoprevention of childhood cancers with higher therapeutic specificity. Considering its significant therapeutic effects in high-risk NB models, the favorable pharmacokinetic and pharmacodynamic profiles, and its high drug-likeness based on Lipinski's rule of five (Table S5), our current lead EP2 antagonist TG6-129 is well positioned as a prime candidate for further development and progression to more intense pre-clinical and clinical studies.

Limitations of the study

The overall effects of pharmacological inhibition of EP2 by TG6-129 on NB growth were not as great as that of either genetic deletion or inducible depletion of the receptor in tumor cells. Therefore, it is highly desired that the potency and pharmacokinetic properties of the compound should be further improved for more robust effects. Moreover, it appears that TG6-129 showed reduced efficacy in suppressing the growth of *MYCN*-amplified NB cells when compared with NB cells with 11q deletion, and this can be explained by the higher aggressiveness of *MYCN*-amplified NB tumors. As such, future studies should also be directed to evaluate the combined treatment of EP2 antagonists and current chemotherapy drugs in *MYCN*-amplified and immunocompetent models of NB.

STAR★METHODS

RESOURCE AVAILABILITY

Lead contact—Further information and requests for resources and reagents should be directed to and will be fulfilled by the lead contact, Jianxiong Jiang (jjiang18@uthsc.edu).

Materials availability—All plasmids and cell lines generated in this study are available from the lead contact upon request with a completed Material Transfer Agreement.

Data and code availability

- All data reported in this study will be shared by the lead contact upon request.

- This paper does not report original code.

- Any additional information required to reanalyze the data reported in this paper is available from the lead contact upon request.

EXPERIMENTAL MODEL AND SUBJECT DETAILS Cell lines

Human NB cell lines SK-N-AS (sex: female), SK-N-SH (sex: female), SH-SY5Y(sex: female), SK-N-BE(2) (sex: male), BE(2)-C (sex: male), IMR-32 (sex: male), mouse NB cell line Neuro-2a (sex: male), and human normal fibroblast cell line Hs68 (sex: male) from the American Type Culture Collection (ATCC) were cultured in Dulbecco's Modified Eagle's medium (DMEM, Gibco) supplemented with 10% (v/v) fetal bovine serum (FBS, HyClone) and penicillin (100 U/mL)/streptomycin (100 μg/mL) (Gibco). Human NB cell lines CHLA-90 (sex: male), CHLA-136 (sex: female), NB-EBc1 (sex: male), and NB-1691 (sex: male) from Childhood Cancer Repository were grown in Iscove's Modified Dulbecco's Medium (Gibco) plus 20% FBS, 4 mM L-glutamine, $1 \times$ ITS (5 μg/m/insulin, 5 μg/mL transferrin, 5 ng/mL selenous acid), and penicillin (100 U/mL)/streptomycin (100 μg/mL). Human NB cell line SiMa (sex: male) was purchased from DSMZ-German Collection of Microorganisms and Cell Cultures and cultured in RPMI 1640 medium (Gibco) with 10% FBS, 2 mM L-glutamine, and penicillin (100 U/mL)/streptomycin (100 μg/mL). Mouse NB cell line NXS2 was obtained from the Scripps Research Institute and cultured in DMEM plus 10% FBS and penicillin (100 U/mL)/streptomycin (100 μg/mL). All cell lines were validated by short tandem repeat (STR) using Promega PowerPlex 16 HS System and were regularly tested for contamination of mycoplasma by e-Myco PCR (Bulldog Bio) and were mycoplasma-free throughout this study. Cells were cultured in a humidified incubator at 37°C with 5% CO_2.

Mice—Athymic nude mice (4–6 weeks, female, Charles River Laboratories or Envigo) and A/J inbred mice (4–6 weeks, female, Jackson Laboratory) were housed under a 12-h light/dark cycle with food and water *ad libitum.* Every effort was made to lessen animal suffering. All animal procedures followed the institutional and IACUC guidelines at the University of Tennessee Health Science Center. To create flank tumors, mice were subcutaneously injected with NB cells mixed with Matrigel while the animals were anesthetized with isoflurane to enable an accurate site of injection. Tumor growth was monitored by measuring tumor volume daily using the formula: $V = (width)^2 \times (length) \times 0.5$. After solid tumors appeared, mice were randomized and treated with either vehicle (4% DMSO +80% PEG 400 + 16% H_2O) or selective EP2 antagonist TG6-129 as indicated in each experiment.

METHOD DETAILS

The gene-expression database R2—Gene-expression analyses of the impact of PGE_2 signaling-associated enzymes and receptors including two cyclooxygenases (COXs), three prostaglandin E synthases (PGESs) and four PGE_2 receptors (EPs) on the overall survival in NB patients were performed using a publicly available database (R2 Genomics Analysis and Visualization Platform: http://r2.amc.nl). The NB patient datasets used in this study include SEQC-498, Kocak-649, Versteeg-88, and Primary NRC-283.

Correlation analysis of gene expression—For correlation analysis of multiple gene expression in human NB samples, mRNA expression data were extracted from the NB datasets on R2 database and analyzed using Pearson correlation coefficient analysis.

Cell-based cAMP assay—Cytosol cAMP was measured using a cell-based homogeneous time-resolved fluorescence resonance energy transfer (TR-FRET) method (Cisbio Bioassays) (Jiang et al., 2010, 2018). The assay is based on the generation of a strong FRET signal upon the interaction of two fluorescent molecules: FRET donor cryptate linked with anti-cAMP antibody and FRET acceptor d2 coupled to cAMP. Endogenous cAMP synthesized by cells upon stimulation competes with fluorescence-labeled cAMP for binding to the cAMP antibody, and thus decreases the FRET signal. Human NB cells or normal control fibroblast cells were seeded into 384-well plates with 40 μl complete medium (~4,000 cells/well) and grown overnight. The medium was completely withdrawn and 10 μl Hanks' Balanced Salt solution (HBSS) supplemented with 20 μM rolipram was added into the wells to block phosphodiesterases that might metabolize cAMP. The cells were incubated at room temperature for 30 min, and then treated with vehicle or tested compounds for 5–10 min before incubation with appropriate agonists for 40 min. The cells were lysed in 10 μL lysis buffer containing the FRET acceptor cAMP-d2 and 1 min later another 10 μL lysis buffer with anti-cAMP-cryptate was added. After incubation for 1 h at room temperature, the FRET signal was measured by a 2104 Envision Multilabel Plate Reader (PerkinElmer) with an excitation at 340/25 nm and dual emissions at 665 nm and 590 nm for d2 and cryptate (100 μs delay), respectively. The FRET signal was expressed as $F665/F590 \times 10^4$.

CRISPR/Cas9-mediated gene knockout—Human NB cell lines lacking the EP2 receptor (EP2$^{-/-}$) were generated by CRISPR/Cas9-based genome editing (Addgene) (Shalem et al., 2014; Zelenay et al., 2015), as we previously described (D'Oto et al., 2021; Hu et al., 2018). To create the EP2 knockout (KO) NB cells, sgRNAs targeting human EP2 genome (EP2 KO1: 5′-CGTACGAAGCCAGTACCACT-3′; EP2 KO2: 5′-GGTCATGGCGAAAGCGAAGT-3′) were cloned into the *BsmB*I sites of lentiCRISPRv2 vector. The 293T cells were transfected with lentiCRISPRv2 (as wild-type control), lentiCRISPRv2_KO1, or lentiCRISPRv2_KO2 along with packaging and envelope plasmids psPAX2 and pMD2.G (w/w/w: 4/3/1) using Lipofectamine 2000. Viral supernatants were harvested 48 h after transfection. Human NB cells SK-N-AS were transduced by lentiviruses using 10 μg/mL polybrene, and cells were then selected under puromycin (2 μg/mL). Targeted clones (EP2$^{-/-}$) were screened and verified by sequencing, qPCR, and cell-based TR-FRET functional assay.

Inducible conditional knockdown of EP2—NB cells with conditional knockdown (KD) of EP2 were generated using Tet-inducible lentiviral shRNA (Horizon Discovery) targeting human EP2 (5′-TGAAGTTTAATCTGGTCTG-3′) as we previously described (Singh et al., 2021). In brief, lentiviral particles were packaged in 293T cells with pTRIPZ-shRNA plasmid and packaging vectors psPAX2 and pMD2.G (w/w/w: 4/3/1) using Lipofectamine 2000. Viral supernatants were harvested 48 h after transfection. Human NB cells SK-N-AS were transduced by lentiviruses using 10 μg/mL polybrene, and cells were then selected under puromycin (2 μg/mL). Expression of EP2 shRNA was induced by treatment with 0.5 μg/mL doxycycline, and the efficacy of EP2 KD was verified by qPCR. To induce EP2 KD in subcutaneous tumors formed by NB cells, mice were treated by

doxycycline (50 mg/kg, i.p.) daily. The efficacy of EP2 KD in tumor tissues was verified by immunohistochemistry.

Quantitative PCR—The mRNA levels of interested genes were quantified by quantitative PCR (qPCR) as described previously (Kang et al., 2017; Li et al., 2020). The total RNA was isolated using TRIzol (Invitrogen) with the PureLink RNA Mini Kit (Invitrogen). RNA purity and concentration were measured by A260/A280 ratio and A260 value, respectively, using a NanoDrop One microvolume spectrophotometer (Thermo Scientific). The first-strand cDNA was synthesized using the SuperScript III First-Strand Synthesis SuperMix (Invitrogen) following the product manual. The qPCR was performed using 8 μl of 10× diluted cDNA, 0.4 μM of primers, and 2× SYBR Green SuperMix with a final volume of 20 μl in a CFX96 Touch Real-Time PCR Detection System (Bio-Rad Laboratories). Cycling conditions were as follows: 95°C for 2 min followed by 40 cycles of 95°C for 15 s and then 60°C for 1 min. Melting curve analysis was used to verify single-species PCR product. Fluorescent data were acquired at the 60°C step. The cycle of quantification for GAPDH was subtracted from the cycle of quantification measured for each gene of interest to yield Cq. Samples without cDNA template served as negative controls. The qPCR primers for human EP2 receptor: forward, 5′-TTGGGTCTTTGCCATCCTTAG-3′; reverse, 5′-AGGAAGTTTGTGTTGCATCTTG-3′. Primers for human GAPDH: forward, 5′-GTCAAGGCTGAGAACGGGAA-3′; reverse, 5′-AAATGAGCCCCAGCCTTCTC-3′.

Neurosphere and colony formation assay—Neurosphere and colony formation assays were performed as we previously described (Yang et al., 2017). For neurosphere formation assay, human NB cells were seeded onto an ultra-low attachment 6-well plate (Corning) with a density of 5×10^4 cells/well. Tested compounds were added to the culture medium directly at concentrations indicated. Neurospheres formed by NB cells typically began to show 72 h after seeding and continued being monitored under a microscope. At the end point of the treatment, the neurospheres were analyzed and diameters were measured using ImageJ software developed by the National Institutes of Health (NIH).

For colony formation assay, cells were seeded in a regular 6-well cell culture plate with a density of 4,000 cells/well. Two days later, cells were treated with tested compounds at concentrations indicated. After 2 weeks, colonies formed by NB cells were fixed using 4% paraformaldehyde (PFA) for 20 min and stained with 0.1% Crystal Violet (Sigma) for 1 h. The stained cells were then washed with ddH$_2$O and scanned. The density of colonies was analyzed and quantified using ImageJ software (NIH).

Immunohistochemistry—Subcutaneous tumors were harvested and sectioned (10 μm) using an HM525 NX Cryostat (Thermo Scientific). The tumor tissue sections were fixed by 4% PFA at room temperature for 15 min and permeabilized with 0.25% Triton X-100 at room temperature for 10 min. After blocking in 10% goat serum in PBS at room temperature for 1 h, the sections were incubated in primary antibodies at 4°C overnight: rabbit anti-Ki-67 (1:200, Biocare Medical, Cat# CRM 325B); rat anti-cluster of differentiation 31 (CD31) (1:200, eBioscience, Cat# 14-0311-82); rabbit anti-EP2 (1:100, Cayman Chemical, Cat# 101750); mouse anti-IL-1β (1:100, Cell Signaling Technology, Cat# 12242S); rabbit anti-IL-6 (1:100, Santa Cruz Biotechnology, Cat# sc-1265); rabbit anti-cleaved caspase-3

(1:200, Cell Signaling Technology, Cat# 9664T); rabbit anti-cleaved PARP (1:200, Cell Signaling Technology, Cat# 5625S). The sections were washed with PBS and incubated with secondary antibodies: goat anti-rabbit IgG-Alexa Fluor 488 (1:1,000, Invitrogen, Cat# A-11034), goat anti-rabbit IgG-Alexa Fluor 546 (1:1,000, Invitrogen, Cat# A-11035), goat anti-mouse IgG-Alexa Fluor 488 (1:1,000, Invitrogen, Cat# A-11001), or goat anti-rat IgG-Alexa Fluor 488 (1:1,000, Invitrogen, Cat# A-11006), at room temperature for 2 h and DAPI (1 μg/mL in PBS) for 10 min. Stained sections were mounted on slides using DPX Mountant (Electron Microscopy Sciences). Images were obtained using a fluorescence microscope BZ-X800 (KEYENCE). The fluorescence intensity was quantified using ImageJ software (NIH).

QUANTIFICATION AND STATISTICAL ANALYSIS

The concentration-response curves of tested agonists and antagonists were generated and EC_{50} and IC_{50} values were calculated using OriginPro software (OriginLab). Statistical analyses were performed using Prism (GraphPad Software) by paired/unpaired *t* test or one-way/two-way ANOVA with *post-hoc* Dunnett's test for multiple comparisons as indicated in each experiment. The correlation analyses were performed using Pearson's correlation coefficient. $p < 0.05$ was considered statistically significant. All data are presented as mean + or ± SEM.

Supplementary Material

Refer to Web version on PubMed Central for supplementary material.

ACKNOWLEDGMENTS

REFERENCES

Aoki T, and Narumiya S (2017). Prostaglandin E2-EP2 signaling as a node of chronic inflammation in the colon tumor microenvironment. Inflamm. Regen 37, 4. 10.1186/s41232-017-0036-7. [PubMed: 29259703]

Ara T, Nakata R, Sheard MA, Shimada H, Buettner R, Groshen SG, Ji L, Yu H, Jove R, Seeger RC, and DeClerck YA (2013). Critical role of STAT3 in IL-6-mediated drug resistance in human neuroblastoma. Cancer Res. 73, 3852–3864. 10.1158/0008-5472.CAN-12-2353. [PubMed: 23633489]

Becker J, Pavlakovic H, Ludewig F, Wilting F, Weich HA, Albuquerque R, Ambati J, and Wilting J (2010). Neuroblastoma progression correlates with downregulation of the lymphangiogenesis inhibitor sVEGFR-2. Clin. Cancer Res. 16, 1431–1441. 10.1158/1078-0432.CCR-09-1936. [PubMed: 20179233]

Carén H, Kryh H, Nethander M, Sjöberg RM, Träger C, Nilsson S, Abrahamsson J, Kogner P, and Martinsson T (2010). High-risk neuroblastoma tumors with 11q-deletion display a poor prognostic, chromosome instability phenotype with later onset. Proc. Natl Acad. Sci. USA 107, 4323–4328. 10.1073/pnas.0910684107. [PubMed: 20145112]

Carlson LM, and Kogner P (2013). Neuroblastoma-related inflammation: may small doses of aspirin be suitable for small cancer patients? OncoImmunology 2, e24658. 10.4161/onci.24658. [PubMed: 24073359]

Carlson LM, Rasmuson A, Idborg H, Segerström L, Jakobsson PJ, Sveinbjörnsson B, and Kogner P (2013). Low-dose aspirin delays an inflammatory tumor progression in vivo in a transgenic mouse model of neuroblastoma. Carcinogenesis 34, 1081–1088. 10.1093/carcin/bgt009. [PubMed: 23349014]

Castriconi R, Dondero A, Bellora F, Moretta L, Castellano A, Locatelli F, Corrias MV, Moretta A, and Bottino C (2013). Neuroblastoma-derived TGF-β1 modulates the chemokine receptor repertoire of human resting NK cells. J. Immunol. 190, 5321–5328. 10.4049/jimmunol.1202693. [PubMed: 23576682]

Cavar S, Jelaši D, Jelasic D, Seiwerth S, Miloševi M, Milosevic M, Hutinec Z, Miši M, and Misic M (2015). Endoglin (CD 105) as a potential prognostic factor in neuroblastoma. Pediatr. Blood Cancer 62, 770–775. 10.1002/pbc.25427. [PubMed: 25683142]

Craig BT, Rellinger EJ, Guo Y, Qiao J, and Chung DH (2016). Growth differentiation factor 15 is a novel regulator of the stem cell-like phenotype in neuroblastoma. J. Am. Coll. Surg 223, S87. 10.1016/j.jamcollsurg.2016.06.171.

D'Oto A, Fang J, Jin H, Xu B, Singh S, Mullasseril A, Jones V, Abu-Zaid A, von Buttlar X, Cooke B, et al. (2021). KDM6B promotes activation of the oncogenic CDK4/6-pRB-E2F pathway by maintaining enhancer activity in MYCN-amplified neuroblastoma. Nat. Commun 12, 7204. 10.1038/s41467-021-27502-2. [PubMed: 34893606]

DeLisser HM, Christofidou-Solomidou M, Strieter RM, Burdick MD, Robinson CS, Wexler RS, Kerr JS, Garlanda C, Merwin JR, Madri JA, and Albelda SM (1997). Involvement of endothelial PECAM-1/CD31 in angiogenesis. Am. J. Pathol 151, 671–677. [PubMed: 9284815]

Donnini S, Finetti F, Solito R, Terzuoli E, Sacchetti A, Morbidelli L, Patrignani P, and Ziche M (2007). EP2 prostanoid receptor promotes squamous cell carcinoma growth through epidermal growth factor receptor transactivation and iNOS and ERK1/2 pathways. Faseb. J 21, 2418–2430. 10.1096/fj.06-7581com. [PubMed: 17384145]

Du Y, Kemper T, Qiu J, and Jiang J (2016). Defining the therapeutic time window for suppressing the inflammatory prostaglandin E2 signaling after status epilepticus. Expert Rev. Neurother 16, 123–130. 10.1586/14737175.2016.1134322. [PubMed: 26689339]

El-Badry OM, Helman LJ, Chatten J, Steinberg SM, Evans AE, and Israel MA (1991). Insulin-like growth factor II-mediated proliferation of human neuroblastoma. J. Clin. Invest 87, 648–657. 10.1172/jci115042. [PubMed: 1991849]

Elaraj DM, Weinreich DM, Varghese S, Puhlmann M, Hewitt SM, Carroll NM, Feldman ED, Turner EM, and Alexander HR (2006). The role of interleukin 1 in growth and metastasis of human cancer xenografts. Clin. Cancer Res. 12, 1088–1096. 10.1158/1078-0432.CCR-05-1603. [PubMed: 16489061]

Finetti F, Solito R, Morbidelli L, Giachetti A, Ziche M, and Donnini S (2008). Prostaglandin E2 regulates angiogenesis via activation of fibroblast growth factor receptor-1. J. Biol. Chem 283, 2139–2146. 10.1074/jbc.M703090200. [PubMed: 18042549]

Ganesh T, Jiang J, Shashidharamurthy R, and Dingledine R (2013). Discovery and characterization of carbamothioylacrylamides as EP2 selective antagonists. ACS Med. Chem. Lett 4, 616–621. 10.1021/ml400112h. [PubMed: 23914286]

George RE, Sanda T, Hanna M, Fröhling S, Ii WL, Zhang J, Ahn Y, Zhou W, London WB, McGrady P, et al. (2008). Activating mutations in ALK provide a therapeutic target in neuroblastoma. Nature 455, 975–978. 10.1038/nature07397. [PubMed: 18923525]

Grivennikov SI, Greten FR, and Karin M (2010). Immunity, inflammation, and cancer. Cell 140, 883–899. 10.1016/j.cell.2010.01.025. [PubMed: 20303878]

Grosser T, Yu Y, and Fitzgerald GA (2010). Emotion recollected in tranquility: lessons learned from the COX-2 saga. Annu. Rev. Med 61, 17–33. 10.1146/annurev-med-011209-153129. [PubMed: 20059330]

Hadjidaniel MD, Muthugounder S, Hung LT, Sheard MA, Shirinbak S, Chan RY, Nakata R, Borriello L, Malvar J, Kennedy RJ, et al. (2017). Tumor-associated macrophages promote neuroblastoma

via STAT3 phosphorylation and up-regulation of c-MYC. Oncotarget 8, 91516–91529. 10.18632/oncotarget.21066. [PubMed: 29207662]

Hansford LM, and Marshall GM (2005). Glial cell line-derived neurotrophic factor (GDNF) family ligands reduce the sensitivity of neuroblastoma cells to pharmacologically induced cell death, growth arrest and differentiation. Neurosci. Lett 389, 77–82. 10.1016/j.neulet.2005.07.034. [PubMed: 16125842]

Hashimoto O, Yoshida M, Koma Y, Yanai T, Hasegawa D, Kosaka Y, Nishimura N, and Yokozaki H (2016). Collaboration of cancer-associated fibroblasts and tumour-associated macrophages for neuroblastoma development. J. Pathol 240, 211–223. 10.1002/path.4769. [PubMed: 27425378]

Hirata T, and Narumiya S (2011). Prostanoid receptors. Chem. Rev 111, 6209–6230. 10.1021/cr200010h. [PubMed: 21819041]

Hishiki T, Nimura Y, Isogai E, Kondo K, Ichimiya S, Nakamura Y, Ozaki T, Sakiyama S, Hirose M, Seki N, et al. (1998). Glial cell line-derived neurotrophic factor/neurturin-induced differentiation and its enhancement by retinoic acid in primary human neuroblastomas expressing c-Ret, GFR alpha-1, and GFR alpha-2. Cancer Res. 58, 2158–2165. [PubMed: 9605760]

Ho R, Minturn JE, Hishiki T, Zhao H, Wang Q, Cnaan A, Maris J, Evans AE, and Brodeur GM (2005). Proliferation of human neuroblastomas mediated by the epidermal growth factor receptor. Cancer Res. 65, 9868–9875. 10.1158/0008-5472.CAN-04-2426. [PubMed: 16267010]

Hsu HH, Lin YM, Shen CY, Shibu MA, Li SY, Chang SH, Lin CC, Chen RJ, Viswanadha VP, Shih HN, and Huang CY (2017). Prostaglandin E2-induced COX-2 expressions via EP2 and EP4 signaling pathways in human LoVo colon cancer cells. Int. J. Mol. Sci 18, 1132. 10.3390/ijms18061132.

Hu D, Jablonowski C, Cheng PH, AlTahan A, Li C, Wang Y, Palmer L, Lan C, Sun B, Abu-Zaid A, et al. (2018). KDM5A regulates a translational program that controls p53 protein expression. iScience 9, 84–100. 10.1016/j.isci.2018.10.012. [PubMed: 30388705]

Huang M, and Weiss WA (2013). Neuroblastoma and MYCN. Cold Spring Harbor perspectives in medicine 3, a014415. 10.1101/cshperspect.a014415. [PubMed: 24086065]

Imamura J, Bartram CR, Berthold F, Harms D, Nakamura H, and Koeffler HP (1993). Mutation of the p53 gene in neuroblastoma and its relationship with N-myc amplification. Cancer Res. 53, 4053–4058. [PubMed: 8358734]

Irwin MS, Naranjo A, Zhang FF, Cohn SL, London WB, Gastier-Foster JM, Ramirez NC, Pfau R, Reshmi S, Wagner E, et al. (2021). Revised neuroblastoma risk classification system: a report from the children's oncology group. J. Clin. Oncol 39, 3229–3241. 10.1200/JCO.21.00278. [PubMed: 34319759]

Jain S, Chakraborty G, Raja R, Kale S, and Kundu GC (2008). Prostaglandin E2 regulates tumor angiogenesis in prostate cancer. Cancer Res. 68, 7750–7759. 10.1158/0008-5472.CAN-07-6689. [PubMed: 18829529]

Jakovljevi G, uli S, Stepan J, Bonevski A, and Seiwerth S (2009). Vascular endothelial growth factor in children with neuroblastoma: a retrospective analysis. J. Exp. Clin. Cancer. Res 28, 143. 10.1186/1756-9966-28-143. [PubMed: 19895696]

Jiang J, and Dingledine R (2013a). Prostaglandin receptor EP2 in the cross-hairs of anti-inflammation, anti-cancer, and neuroprotection. Trends Pharmacol. Sci 34, 413–423. 10.1016/j.tips.2013.05.003. [PubMed: 23796953]

Jiang J, and Dingledine R (2013b). Role of prostaglandin receptor EP2 in the regulations of cancer cell proliferation, invasion, and inflammation. J Pharmacol Exp Ther 344, 360–367. 10.1124/jpet.112.200444. [PubMed: 23192657]

Jiang J, Ganesh T, Du Y, Quan Y, Serrano G, Qui M, Speigel I, Rojas A, Lelutiu N, and Dingledine R (2012). Small molecule antagonist reveals seizure-induced mediation of neuronal injury by prostaglandin E2 receptor subtype EP2. Proc. Natl. Acad. Sci. USA 109, 3149–3154. 10.1073/pnas.1120195109. [PubMed: 22323596]

Jiang J, Ganesh T, Du Y, Thepchatri P, Rojas A, Lewis I, Kurtkaya S, Li L, Qui M, Serrano G, et al. (2010). Neuroprotection by selective allosteric potentiators of the EP2 prostaglandin receptor. Proc. Natl. Acad. Sci. USA 107, 2307–2312. 10.1073/pnas.0909310107. [PubMed: 20080612]

Jiang J, Qiu J, Li Q, and Shi Z (2017). Prostaglandin E2 signaling: alternative target for glioblastoma? Trends in cancer 3, 75–78. 10.1016/j.trecan.2016.12.002. [PubMed: 28718447]

Jiang J, Quan Y, Ganesh T, Pouliot WA, Dudek FE, and Dingledine R (2013). Inhibition of the prostaglandin receptor EP2 following status epilepticus reduces delayed mortality and brain inflammation. Proc. Natl. Acad. Sci. USA 110, 3591–3596. 10.1073/pnas.1218498110. [PubMed: 23401547]

Jiang J, Van TM, Ganesh T, and Dingledine R (2018). Discovery of 2-piperidinyl phenyl benzamides and trisubstituted pyrimidines as positive allosteric modulators of the prostaglandin receptor EP2. ACS Chem. Neurosci. 9, 699–707. 10.1021/acschemneuro.7b00486. [PubMed: 29292987]

Kamiyama M, Pozzi A, Yang L, DeBusk LM, Breyer RM, Lin PC, and Pozzi A (2006). EP2, a receptor for PGE_2, regulates tumor angiogenesis through direct effects on endothelial cell motility and survival. Oncogene 25, 7019–7028. 10.1038/sj.onc.1209694. [PubMed: 16732324]

Kang X, Qiu J, Li Q, Bell KA, Du Y, Jung DW, Lee JY, Hao J, and Jiang J (2017). Cyclooxygenase-2 contributes to oxidopamine-mediated neuronal inflammation and injury via the prostaglandin E2 receptor EP2 subtype. Sci. Rep 7, 9459. 10.1038/s41598-017-09528-z. [PubMed: 28842681]

Khan M, Engström C, Fagman JB, Smedh U, Lundholm K, Iresjö BM, and Iresjo BM (2022). Reduced tumor growth in EP2 knockout mice is related to signaling pathways favoring an increased local antitumor immunity in the tumor stroma. Oncol. Rep 47, 118. 10.3892/or.2022.8329. [PubMed: 35543149]

Kock A, Bergqvist F, Steinmetz J, Elfman LHM, Korotkova M, Johnsen JI, Jakobsson PJ, Kogner P, and Larsson K (2020). Establishment of an in vitro 3D model for neuroblastoma enables preclinical investigation of combined tumor-stroma drug targeting. Faseb. J 34, 11101–11114. 10.1096/fj.202000684R. [PubMed: 32623799]

Kock A, Larsson K, Bergqvist F, Eissler N, Elfman LHM, Raouf J, Korotkova M, Johnsen JI, Jakobsson PJ, and Kogner P (2018). Inhibition of microsomal prostaglandin E synthase-1 in cancer-associated fibroblasts suppresses neuroblastoma tumor growth. EBioMedicine 32, 84–92. 10.1016/j.ebiom.2018.05.008. [PubMed: 29804818]

Larsson K, Kock A, Idborg H, Arsenian Henriksson M, Martinsson T, Johnsen JI, Korotkova M, Kogner P, and Jakobsson PJ (2015). COX/mPGES-1/PGE2 pathway depicts an inflammatory-dependent high-risk neuroblastoma subset. Proc. Natl. Acad. Sci. USA 112, 8070–8075. 10.1073/pnas.1424355112. [PubMed: 26080408]

Li L, Yasmen N, Hou R, Yang S, Lee JY, Hao J, Yu Y, and Jiang J (2022). Inducible prostaglandin E synthase as a pharmacological target for ischemic stroke. Neurotherapeutics 19, 366–385. 10.1007/s13311-022-01191-1. [PubMed: 35099767]

Li L, Yu Y, Hou R, Hao J, and Jiang J (2020). Inhibiting the PGE2 receptor EP2 mitigates excitotoxicity and ischemic injury. ACS Pharmacol Transl Sci 3, 635–643. 10.1021/acsptsci.0c00040. [PubMed: 32832866]

Liberman J, Sartelet H, Flahaut M, Mühlethaler-Mottet A, Coulon A, Nyalendo C, Vassal G, Joseph JM, and Gross N (2012). Involvement of the CXCR7/CXCR4/CXCL12 axis in the malignant progression of human neuroblastoma. PLoS One 7, e43665. 10.1371/journal.pone.0043665. [PubMed: 22916293]

Lode HN, Xiang R, Varki NM, Dolman CS, Gillies SD, and Reisfeld RA (1997). Targeted interleukin-2 therapy for spontaneous neuroblastoma metastases to bone marrow. J. Natl. Cancer Inst 89, 1586–1594. 10.1093/jnci/89.21.1586. [PubMed: 9362156]

Ma X, Aoki T, Tsuruyama T, and Narumiya S (2015). Definition of prostaglandin E2-EP2 signals in the colon tumor microenvironment that amplify inflammation and tumor growth. Cancer Res. 75, 2822–2832. 10.1158/0008-5472.CAN-15-0125. [PubMed: 26018088]

Ma X, Kundu N, Collin PD, Goloubeva O, and Fulton AM (2012). Frondoside A inhibits breast cancer metastasis and antagonizes prostaglandin E receptors EP4 and EP2. Breast Cancer Res. Treat 132, 1001–1008. 10.1007/s10549-011-1675-z. [PubMed: 21761157]

Mantovani A, Allavena P, Sica A, and Balkwill F (2008). Cancer-related inflammation. Nature 454, 436–444. 10.1038/nature07205. [PubMed: 18650914]

Maris JM (2010). Recent advances in neuroblastoma. N. Engl. J. Med 362, 2202–2211. 10.1056/NEJMra0804577. [PubMed: 20558371]

Matthay KK, Maris JM, Schleiermacher G, Nakagawara A, Mackall CL, Diller L, and Weiss WA (2016). Neuroblastoma. Nat. Rev. Dis. Primers 2, 16078. 10.1038/nrdp.2016.78. [PubMed: 27830764]

Merz C, von Mässenhausen A, Queisser A, Vogel W, Andrén O, Kirfel J, Duensing S, Perner S, and Nowak M (2016). IL-6 overexpression in ERG-positive prostate cancer is mediated by prostaglandin receptor EP2. Am. J. Pathol 186, 974–984. 10.1016/j.ajpath.2015.12.009. [PubMed: 27012192]

Metelitsa LS, Wu HW, Wang H, Yang Y, Warsi Z, Asgharzadeh S, Groshen S, Wilson SB, and Seeger RC (2004). Natural killer T cells infiltrate neuroblastomas expressing the chemokine CCL2. J. Exp. Med. 199, 1213–1221. 10.1084/jem.20031462. [PubMed: 15123743]

Middlemas DS, Kihl BK, Zhou J, and Zhu X (1999). Brain-derived neurotrophic factor promotes survival and chemoprotection of human neuroblastoma cells. J. Biol. Chem 274, 16451–16460. 10.1074/jbc.274.23.16451. [PubMed: 10347207]

Mlakar V, Jurkovic Mlakar S, Lopez G, Maris JM, Ansari M, and Gumy-Pause F (2017). 11q deletion in neuroblastoma: a review of biological and clinical implications. Mol. Cancer 16, 114. 10.1186/s12943-017-0686-8. [PubMed: 28662712]

Mohlin S, Hamidian A, and Påhlman S (2013). HIF2A and IGF2 expression correlates in human neuroblastoma cells and normal immature sympathetic neuroblasts. Neoplasia 15, 328–IN38. 10.1593/neo.121706. [PubMed: 23479510]

Mossé YP, Laudenslager M, Longo L, Cole KA, Wood A, Attiyeh EF, Laquaglia MJ, Sennett R, Lynch JE, Perri P, et al. (2008). Identification of ALK as a major familial neuroblastoma predisposition gene. Nature 455, 930–935. 10.1038/nature07261. [PubMed: 18724359]

Nakanishi M, and Rosenberg DW (2013). Multifaceted roles of PGE2 in inflammation and cancer. Semin. Immunopathol 35, 123–137. 10.1007/s00281-012-0342-8. [PubMed: 22996682]

Nevo I, Sagi-Assif O, Meshel T, Ben-Baruch A, Jöhrer K, Greil R, Trejo LEL, Kharenko O, Feinmesser M, Yron I, and Witz IP (2009). The involvement of the fractalkine receptor in the transmigration of neuroblastoma cells through bone-marrow endothelial cells. Cancer Lett. 273, 127–139. 10.1016/j.canlet.2008.07.029. [PubMed: 18778890]

Nyalendo C, Sartelet H, Barrette S, Ohta S, Gingras D, and Béliveau R (2009). Identification of membrane-type 1 matrix metalloproteinase tyrosine phosphorylation in association with neuroblastoma progression. BMC Cancer 9, 422. 10.1186/1471-2407-9-422. [PubMed: 19961596]

O'Brien AJ, Fullerton JN, Massey KA, Auld G, Sewell G, James S, Newson J, Karra E, Winstanley A, Alazawi W, et al. (2014). Immunosuppression in acutely decompensated cirrhosis is mediated by prostaglandin E2. Nat. Med 20, 518–523. 10.1038/nm.3516. [PubMed: 24728410]

O'Brien R, Tran SL, Maritz MF, Liu B, Kong CF, Purgato S, Yang C, Murray J, Russell AJ, Flemming CL, et al. (2016). MYC-driven neuroblastomas are addicted to a telomerase-independent function of dyskerin. Cancer Res. 76, 3604–3617. 10.1158/0008-5472.CAN-15-0879. [PubMed: 27197171]

O'Callaghan G, and Houston A (2015). Prostaglandin E2 and the EP receptors in malignancy: possible therapeutic targets? Br. J. Pharmacol 172, 5239–5250. 10.1111/bph.13331. [PubMed: 26377664]

Okuyama T, Ishihara S, Sato H, Rumi MA, Kawashima K, Miyaoka Y, Suetsugu H, Kazumori H, Cava CF, Kadowaki Y, et al. (2002). Activation of prostaglandin E2-receptor EP2 and EP4 pathways induces growth inhibition in human gastric carcinoma cell lines. J. Lab. Clin. Med 140, 92–102. 10.1067/mlc.2002.125784. [PubMed: 12228765]

Pezzolo A, Parodi F, Corrias MV, Cinti R, Gambini C, and Pistoia V (2007). Tumor origin of endothelial cells in human neuroblastoma. J. Clin. Oncol 25, 376–383. 10.1200/JCO.2006.09.0696. [PubMed: 17264333]

Pistoia V, Bianchi G, Borgonovo G, and Raffaghello L (2011). Cytokines in neuroblastoma: from pathogenesis to treatment. Immunotherapy 3, 895–907. 10.2217/imt.11.80. [PubMed: 21751957]

Qiu J, Li Q, Bell KA, Yao X, Du Y, Zhang E, Yu JJ, Yu Y, Shi Z, and Jiang J (2019). Small-molecule inhibition of prostaglandin E receptor 2 impairs cyclooxygenase-associated malignant glioma growth. Br. J. Pharmacol 176, 1680–1699. 10.1111/bph.14622. [PubMed: 30761522]

Qiu J, Shi Z, and Jiang J (2017). Cyclooxygenase-2 in glioblastoma multiforme. Drug Discov. Today 22, 148–156. 10.1016/j.drudis.2016.09.017. [PubMed: 27693715]

Quan Y, Jiang J, and Dingledine R (2013). EP2 receptor signaling pathways regulate classical activation of microglia. J. Biol. Chem 288, 9293–9302. 10.1074/jbc.M113.455816. [PubMed: 23404506]

Rasmuson A, Kock A, Fuskevåg OM, Kruspig B, Simón-Santamaría J, Gogvadze V, Johnsen JI, Kogner P, and Sveinbjörnsson B (2012). Auto-crine prostaglandin E2 signaling promotes tumor cell survival and proliferation in childhood neuroblastoma. PLoS One 7, e29331. 10.1371/journal.pone.0029331. [PubMed: 22276108]

Rossi A, Granata F, Augusti-Tocco G, Canu N, Levi A, and Possenti R (1992). Expression in murine and human neuroblastoma cell lines of VGF, a tissue specific protein. Int. J. Dev. Neurosci 10, 527–534. 10.1016/0736-5748(92)90053-3. [PubMed: 1288062]

Rossler J, Taylor M, Geoerger B, Farace F, Lagodny J, Peschka-Suss R, Niemeyer CM, and Vassal G (2008). Angiogenesis as a target in neuroblastoma. European. J. Cancer 44, 1645–1656. 10.1016/j.ejca.2008.05.015. [PubMed: 18614349]

Roy Choudhury S, Karmakar S, Banik NL, and Ray SK (2012). Targeting angiogenesis for controlling neuroblastoma. J. Oncol 2012, 1–15. 10.1155/2012/782020.

Rundhaug JE, Simper MS, Surh I, and Fischer SM (2011). The role of the EP receptors for prostaglandin E2 in skin and skin cancer. Cancer Metastasis Rev. 30, 465–480. 10.1007/s10555-011-9317-9. [PubMed: 22012553]

Samuelsson B, Morgenstern R, and Jakobsson PJ (2007). Membrane prostaglandin E synthase-1: a novel therapeutic target. Pharmacol. Rev 59, 207–224. 10.1124/pr.59.3.1. [PubMed: 17878511]

Sasaki H, Sato Y, Kondo S, Fukai I, Kiriyama M, Yamakawa Y, and Fuji Y (2002). Expression of the periostin mRNA level in neuroblastoma. J. Pediatr. Surg 37, 1293–1297. 10.1053/jpsu.2002.34985. [PubMed: 12194119]

Shalem O, Sanjana NE, Hartenian E, Shi X, Scott DA, Mikkelsen TS, Heckl D, Ebert BL, Root DE, Doench JG, and Zhang F (2014). Genome-scale CRISPR-Cas9 knockout screening in human cells. Science (New York, N.Y.) 343, 84–87. 10.1126/science.1247005.

Singh S, Quarni W, Goralski M, Wan S, Jin H, Van de Velde LA, Fang J, Wu Q, Abu-Zaid A, Wang T, et al. (2021). Targeting the spliceosome through RBM39 degradation results in exceptional responses in high-risk neuroblastoma models. Sci. Adv 7, eabj5405. 10.1126/sciadv.abj5405. [PubMed: 34788094]

Sluter MN, Hou R, Li L, Yasmen N, Yu Y, Liu J, and Jiang J (2021). EP2 antagonists (2011-2021): a decade's journey from discovery to therapeutics. J. Med. Chem 64, 11816–11836. 10.1021/acs.jmedchem.1c00816. [PubMed: 34352171]

Spel L, Schiepers A, and Boes M (2018). NFκB and MHC-1 interplay in neuroblastoma and immunotherapy. Trends Cancer 4, 715–717. 10.1016/j.trecan.2018.09.006. [PubMed: 30352674]

Spinella F, Rosanò L, Di Castro V, Natali PG, and Bagnato A (2004). Endothelin-1-induced prostaglandin E2-EP2, EP4 signaling regulates vascular endothelial growth factor production and ovarian carcinoma cell invasion. J. Biol. Chem 279, 46700–46705. 10.1074/jbc.M408584200. [PubMed: 15347673]

Stermann A, Huebener N, Seidel D, Fest S, Eschenburg G, Stauder M, Schramm A, Eggert A, and Lode HN (2015). Targeting of MYCN by means of DNA vaccination is effective against neuroblastoma in mice. Cancer Immunol. Immunother 64, 1215–1227. 10.1007/s00262-015-1733-1. [PubMed: 26076666]

Sugiura Y, Shimada H, Seeger RC, Laug WE, and DeClerck YA (1998). Matrix metalloproteinases-2 and -9 are expressed in human neuroblastoma: contribution of stromal cells to their production and correlation with metastasis. Cancer Res. 58, 2209–2216. [PubMed: 9605768]

Sung YM, He G, and Fischer SM (2005). Lack of expression of the EP2 but not EP3 receptor for prostaglandin E2 results in suppression of skin tumor development. Cancer Res. 65, 9304–9311. 10.1158/0008-5472.Can-05-1015. [PubMed: 16230392]

Trau HA, Brännström M, Curry TE Jr., and Duffy DM (2016). Prostaglandin E2 and vascular endothelial growth factor a mediate angiogenesis of human ovarian follicular endothelial cells. Human Reprod. 31, 436–444. 10.1093/humrep/dev320.

Trigg RM, and Turner SD (2018). ALK in neuroblastoma: biological and therapeutic implications. Cancers 10, 113. 10.3390/cancers10040113.

Tümmler C, Snapkov I, Wickström M, Moens U, Ljungblad L, Maria Elfman, L.H., Winberg JO, Kogner P, Johnsen JI, and Sveinbjørnsson B (2017). Inhibition of chemerin/CMKLR1 axis in neuroblastoma cells reduces clonogenicity and cell viability in vitro and impairs tumor growth in vivo. Oncotarget 8, 95135–95151. 10.18632/oncotarget.19619. [PubMed: 29221117]

Tweddle DA, Pearson AD, Haber M, Norris MD, Xue C, Flemming C, and Lunec J (2003). The p53 pathway and its inactivation in neuroblastoma. Cancer Lett. 197, 93–98. 10.1016/s0304-3835(03)00088-0. [PubMed: 12880966]

Van Maerken T, Rihani A, Dreidax D, De Clercq S, Yigit N, Marine JC, Westermann F, De Paepe A, Vandesompele J, and Speleman F (2011). Functional analysis of the p53 pathway in neuroblastoma cells using the small-molecule MDM2 antagonist nutlin-3. Mol. Cancer Therapeut. 10, 983–993. 10.1158/1535-7163.MCT-10-1090.

Wang D, and Dubois RN (2010). Eicosanoids and cancer. Nat. Rev. Cancer 10, 181–193. 10.1038/nrc2809. [PubMed: 20168319]

Wang D, and DuBois RN (2016). The role of prostaglandin E(2) in tumor-associated immunosuppression. Trends Mol. Med 22, 1–3. 10.1016/j.molmed.2015.11.003. [PubMed: 26711015]

Wang J, Zhang L, Kang D, Yang D, and Tang Y (2018). Activation of PGE2/EP2 and PGE2/EP4 signaling pathways positively regulate the level of PD-1 in infiltrating CD8(+) T cells in patients with lung cancer. Oncol. Lett 15, 552–558. 10.3892/ol.2017.7279. [PubMed: 29285200]

Webb MW, Sun J, Sheard MA, Liu WY, Wu HW, Jackson JR, Malvar J, Sposto R, Daniel D, and Seeger RC (2018). Colony stimulating factor 1 receptor blockade improves the efficacy of chemotherapy against human neuroblastoma in the absence of T lymphocytes. Int. J. Cancer 143, 1483–1493. 10.1002/ijc.31532. [PubMed: 29665011]

Weng WC, Lin KH, Wu PY, Ho YH, Liu YL, Wang BJ, Chen CC, Lin YC, Liao YF, Lee WT, et al. (2017). VEGF expression correlates with neuronal differentiation and predicts a favorable prognosis in patients with neuroblastoma. Sci. Rep 7, 11212. 10.1038/s41598-017-11637-8. [PubMed: 28894229]

Wu HW, Sheard MA, Malvar J, Fernandez GE, DeClerck YA, Blavier L, Shimada H, Theuer CP, Sposto R, and Seeger RC (2019). Anti-CD105 antibody eliminates tumor microenvironment cells and enhances anti-GD2 antibody immunotherapy of neuroblastoma with activated natural killer cells. Clin. Cancer Res. 25, 4761–4774. 10.1158/1078-0432.CCR-18-3358. [PubMed: 31068371]

Yang J, Milasta S, Hu D, AlTahan AM, Interiano RB, Zhou J, Davidson J, Low J, Lin W, Bao J, et al. (2017). Targeting histone demethylases in MYC-driven neuroblastomas with ciclopirox. Cancer Res. 77, 4626–4638. 10.1158/0008-5472.CAN-16-0826. [PubMed: 28684529]

Yu Y, Ricciotti E, Scalia R, Tang SY, Grant G, Yu Z, Landesberg G, Crichton I, Wu W, Pure E, et al. (2012). Vascular COX-2 modulates blood pressure and thrombosis in mice. Sci. Transl. Med 4, 132ra54. 10.1126/scitranslmed.3003787.

Zelenay S, van der Veen AG, Böttcher J, Snelgrove KJ, Rogers N, Acton SE, Chakravarty P, Girotti MR, Marais R, Quezada SA, et al. (2015). Cyclooxygenase-dependent tumor growth through evasion of immunity. Cell 162, 1257–1270. 10.1016/j.cell.2015.08.015. [PubMed: 26343581]

Zhi Y, Duan Y, Zhou X, Yin X, Guan G, Zhang H, Dong Q, and Yang K (2014). NF-κB signaling pathway confers neuroblastoma cells migration and invasion ability via the regulation of CXCR4. Med. Sci. Monit 20, 2746–2752. 10.12659/msm.892597. [PubMed: 25527973]

Zhi Y, Lu H, Duan Y, Sun W, Guan G, Dong Q, and Yang C (2015). Involvement of the nuclear factor-κB signaling pathway in the regulation of CXC chemokine receptor-4 expression in neuroblastoma cells induced by tumor necrosis factor-α. Int. J. Mol. Med 35, 349–357. 10.3892/ijmm.2014.2032. [PubMed: 25503960]

Zimmerman MW, Liu Y, He S, Durbin AD, Abraham BJ, Easton J, Shao Y, Xu B, Zhu S, Zhang X, et al. (2018). MYC drives a subset of high-risk pediatric neuroblastomas and is activated through mechanisms including enhancer hijacking and focal enhancer amplification. Cancer Discov. 8, 320–335. 10.1158/2159-8290.CD-17-0993. [PubMed: 29284669]

Highlights

- EP2 is a leading $G\alpha_s$-coupled receptor for PGE_2-initiated cAMP signaling in NB cells

- Genetic deficiency of EP2 prevents the development and progression of high-risk NB

- Treatment with our EP2 antagonist TG6-129 impairs NB with high-risk genetic factors

- EP2 inhibition shows anti-inflammatory, antiangiogenic, and apoptotic effects in NB
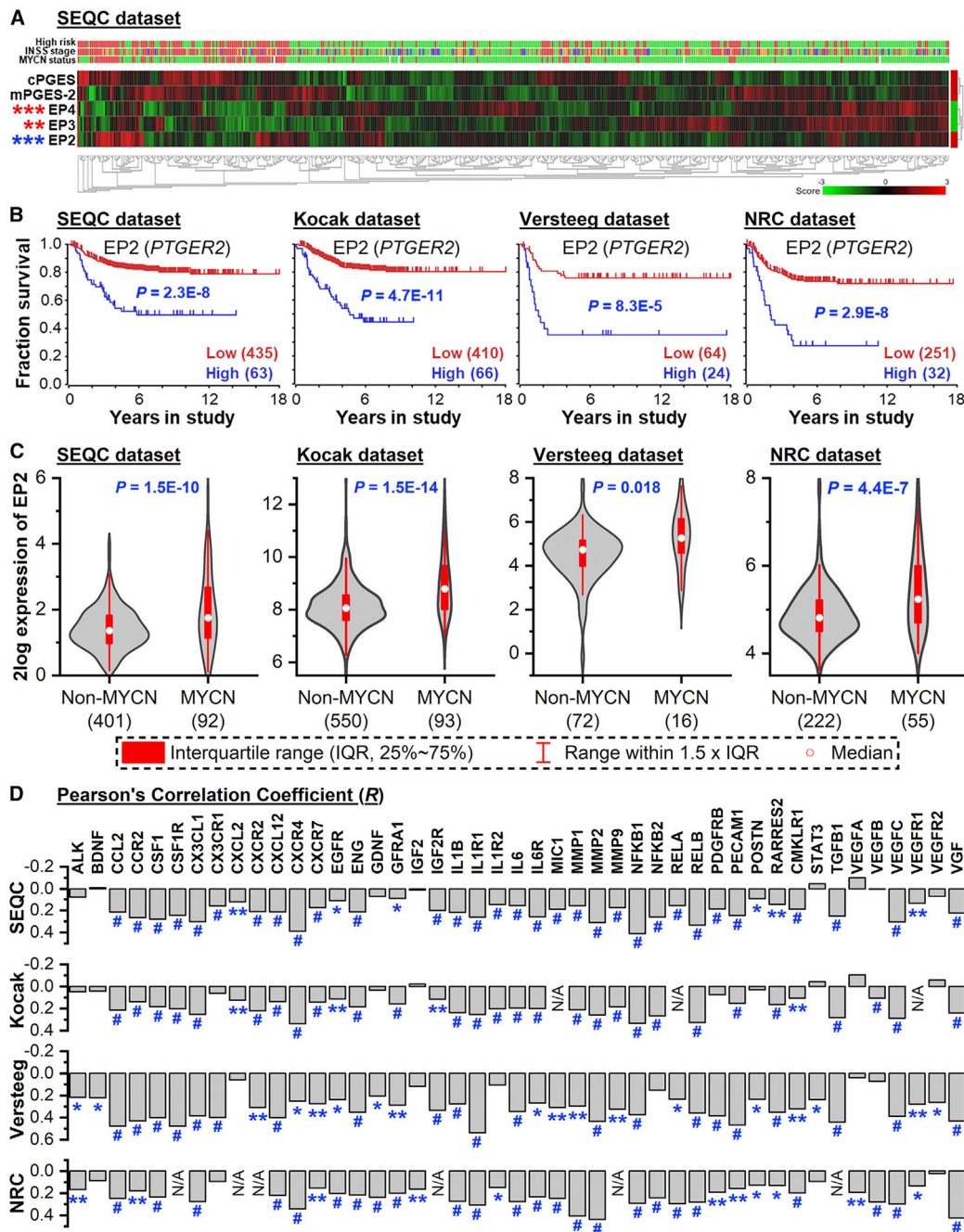
**Figure 1. PGE$_2$ receptor EP2 is highly associated with high-risk NB**

(A) Heatmap analyses of R2 NB patient dataset SEQC (N = 498) reveal that, among all PGE$_2$-related enzymes and receptors, including COX-1 (encoded by *PTGS1*), COX-2 (*PTGS2*), mPGES-1 (*PTGES*), mPGES-2 (*PTGES2*), cPGES (*PTGES3*), EP1 (*PTGER1*), EP2 (*PTGER2*), EP3 (*PTGER3*), and EP4 (*PTGER4*), expression of EP2 receptor shows the highest increase (***p = 5.1E–5, ANOVA) in tumors of nonsurvival patients (N = 105) compared with survival patients (N = 393). Conversely, EP3 and EP4 are downregulated in nonsurvival patients (**p = 0.0028 and ***p = 6.4E–8, respectively, ANOVA).

(B) Patients with high EP2 expression show poorer overall survival across all four major NB datasets in the R2 database, SEQC (p = 2.3E–8, N = 498), Kocak (p = 4.7E–11, N = 476), Versteeg (p = 8.3E–5, N = 88), and NRC (p = 2.9E–8, N = 283), analyzed by Kaplan-Meier estimator with *post hoc* log rank test.

(C) Violin plot with box reveals the differential expression of the EP2 in NB with or without high-risk factor *MYCN* amplification in patients (p = 1.5E–10 in SEQC dataset; p = 1.5E–14 in Kocak; p = 0.018 in Versteeg; p = 4.4E–7 in NRC, t test).

(D) EP2 highly correlates with tumor-promoting cytokines, chemokines, growth factors, and their receptors across all four major NB datasets in the R2 database (*p < 0.05; **p < 0.01; [#]p < 0.001, Pearson's correlation coefficient analysis).

INSS, International Neuroblastoma Staging System; N/A, data not available.
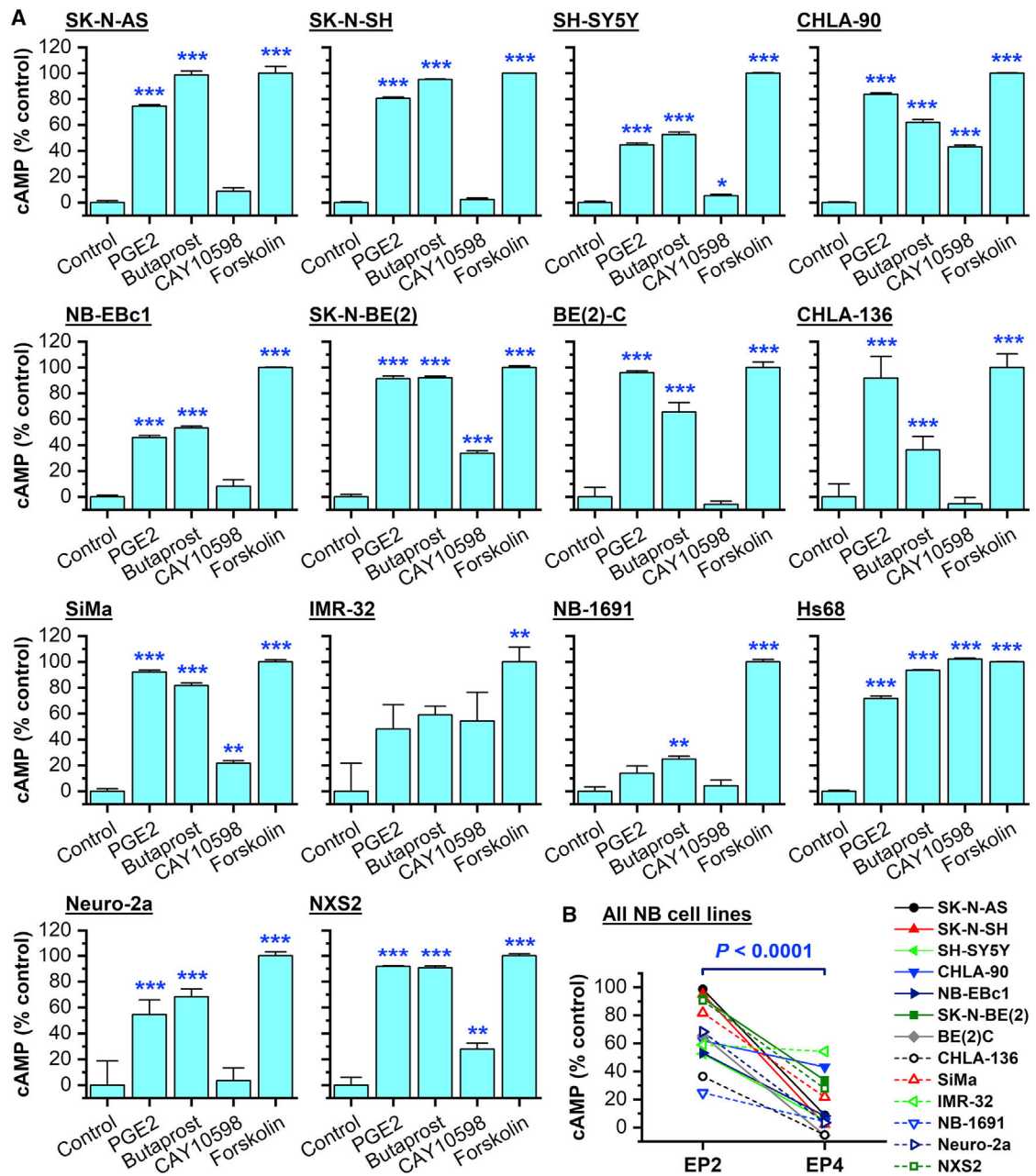
Figure 2. PGE₂ dominantly mediates cAMP signaling in NB cells

(A) Human NB cell lines (SK-N-AS, SK-N-SH, SH-SY5Y, CHLA-90, NB-EBc1, SK-N-BE(2), BE(2)-C, CHLA-136, SiMa, IMR-32, NB-1691), human fibroblast cell line Hs68, and mouse NB cell lines (Neuro-2a and NXS2) were treated with PGE₂ (10 μM), selective EP2 agonist butaprost (10 μM), EP4 agonist CAY10598 (10 μM), or forskolin (100 μM) as positive control. The cAMP signaling in these cells was detected by a TR-FRET method (n = 4–6, *p < 0.05; **p < 0.01; ***p < 0.001, compared with the control group, one-way ANOVA and *post hoc* Dunnett's test). Data are presented as mean + SEM.

(B) The cAMP production via EP2 receptor activation by butaprost and EP4 activation by CAY10598 in all 13 NB cell lines was compared (p < 0.0001, two-tailed paired t test).
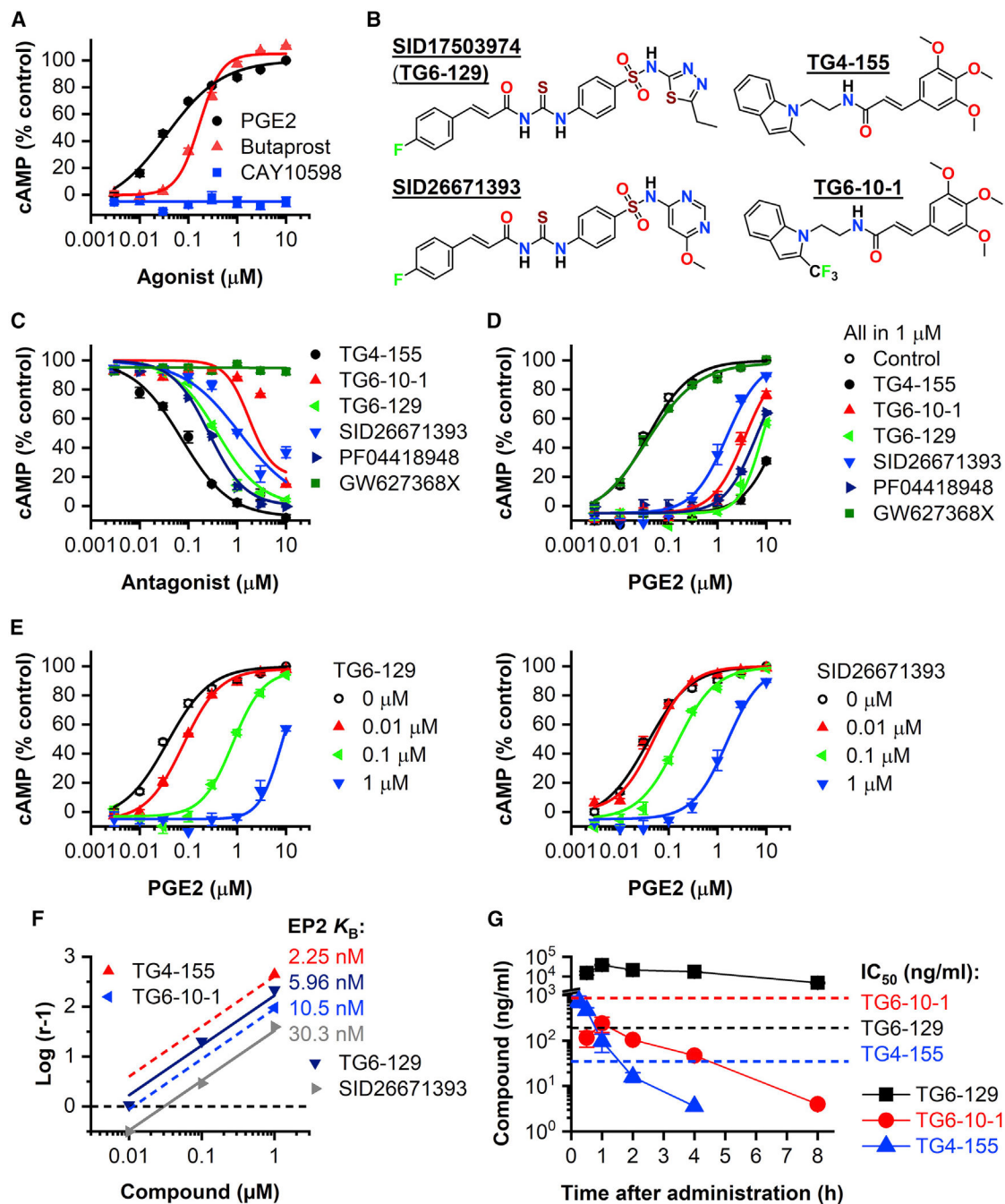
Figure 3. EP2 is the main receptor for PGE$_2$/cAMP signaling in NB cells

(A) PGE$_2$ and EP2 agonist butaprost, but not EP4 agonist CAY10598, induced cAMP in human 11q-deleted NB cell line SK-N-AS in a concentration-dependent manner (n = 4). The calculated PGE$_2$ half maximal effective concentration (EC$_{50}$) was 0.04 μM and butaprost EC$_{50}$ was 0.17 μM. Data are presented as mean ± SEM.

(B) Chemical structures of our EP2 antagonists: TG4-155, TG6-10-1, TG6-129 (SID17503974), and SID26671393.

(C) EP2 antagonists TG4-155, TG6-10-1, TG6-129, SID26671393, and PF04418948, but not EP4 antagonist GW627368X, inhibited 1 μM PGE_2-induced cAMP production in human NB cell line SK-N-AS in a concentration-dependent manner (n = 4). The half maximal inhibitory concentration (IC_{50}) values: 0.07 μM for TG4-155; 1.75 μM for TG6-10-1; 0.39 μM for TG6-129; 1.13 μM for SID26671393; 0.26 μM for PF04418948. Data are presented as mean ± SEM.

(D) TG4-155, TG6-10-1, TG6-129, SID26671393, and PF04418948 (all 1 μM) showed robust inhibition on PGE_2-induced cAMP production in SK-N-AS cells (n = 4). PGE_2 EC_{50} values: 0.04 μM for control; 16.81 μM for TG4-155; 3.65 μM for TG6-10-1; 8.22 μM for TG6-129; 1.54 μM for SID26671393; 6.17 μM for PF04418948. Data are presented as mean ± SEM.

(E) TG6-129 (left) and SID26671393 (right) inhibited PGE_2-induced EP2 activation in SK-N-AS cells in a concentration-dependent manner (n = 4). PGE_2 EC_{50} values: 0.04 μM for control; 0.08, 0.81, and 8.22 μM for 0.01, 0.1, and 1 μM TG6-129, respectively; 0.05, 0.15, and 1.54 μM for 0.01, 0.1, and 1 μM SID26671393, respectively. Data are presented as mean ± SEM.

(F) Tested compounds inhibited EP2 in SK-N-AS cells via a competitive mechanism confirmed by Schild regression analyses (n = 4). TG4-155 K_B: 2.25 nM; TG6-10-1 K_B: 10.5 nM; TG6-129 K_B: 5.96 nM; SID26671393 K_B: 30.3 nM.

(G) After administration in mice (5 mg/kg i.p.), TG6-129, TG6-10-1, and TG4-155 showed plasma half-life: 2.7, 1.6, and 0.6 h (n = 3). Note that the compound IC_{50} values for the EP2 receptor in NB cell line SK-N-AS are also indicated: 192 ng/mL or 390 nM for TG6-129, 34.4 ng/mL or 70 nM for TG4-155, and 862 ng/mL or 1.75 μM for TG6-10-1. Data are presented as mean ± SEM.
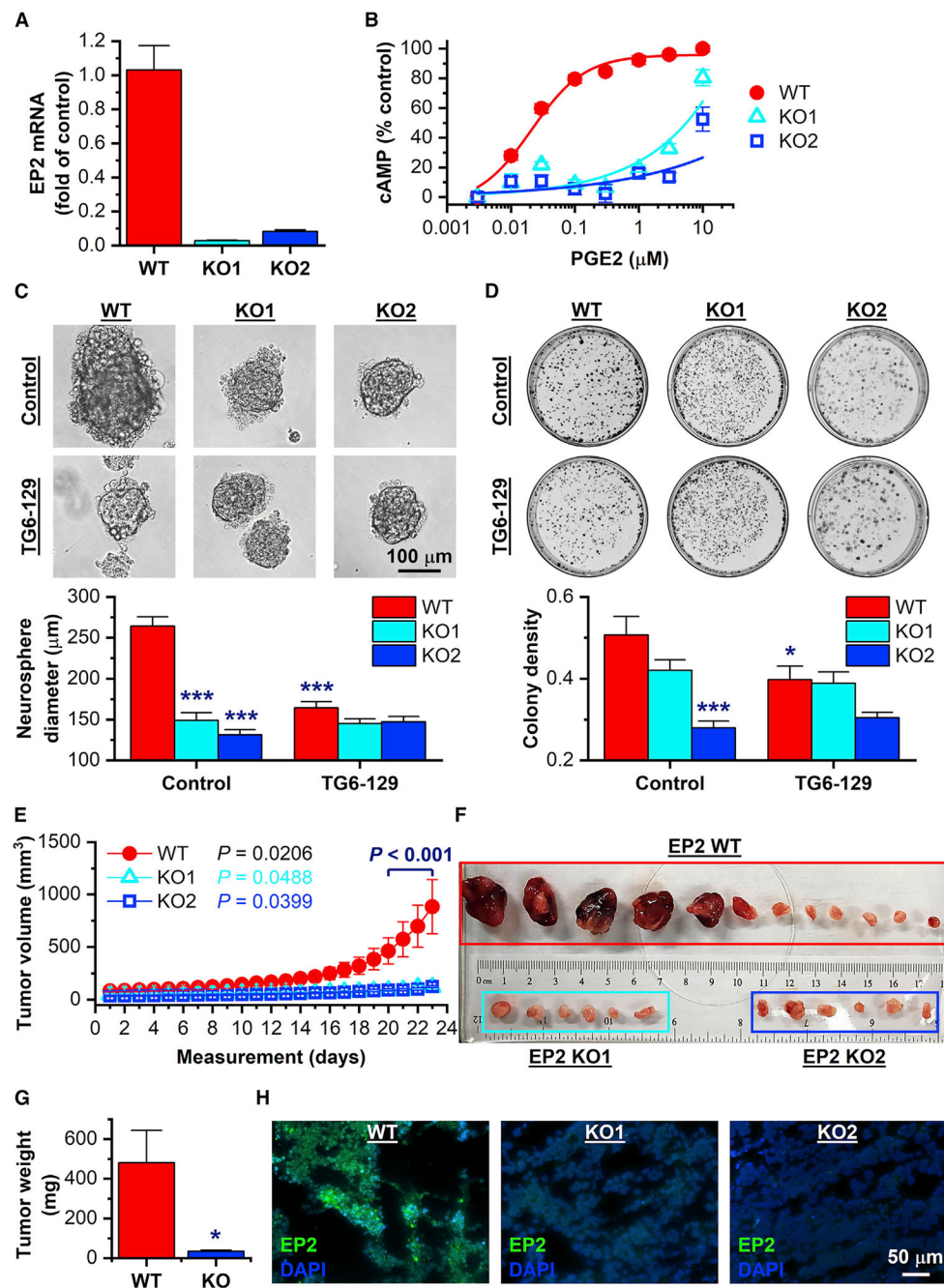
Figure 4. Genetic deletion of EP2 receptor in human NB cells diminishes tumorigenesis

(A) CRISPR-Cas9-generated EP2 deletion in SK-N-AS cells was validated by qPCR. EP2 mRNA expression was detected in the wild-type (WT) cell line, but not in the two knockout (KO) cell lines (KO1 and KO2) (n = 5). Data are presented as mean + SEM.

(B) The WT and KO cell lines were treated by PGE_2, and cAMP levels in these cells were measured by TR-FRET (n = 4). The calculated PGE_2 EC_{50} was 21 nM for the WT cell line and >10 μM for KO1 and KO2 cell lines. Data are presented as mean ± SEM.

(C) EP2 deletion by CRISPR-Cas9 or EP2 inhibition by TG6-129 (10 μM) decreased the size of neurospheres formed by SK-N-AS cells, measured 7 days after seeding (n = 7, *F*

$(5, 36) = 37.11$; $p < 0.0001$; multiple comparisons: ***$p < 0.001$ compared with control, one-way ANOVA with *post hoc* Dunnett's multiple comparisons test). Data are presented as mean + SEM.

(D) EP2 deletion or treatment with TG6-129 (10 μM) for 2 weeks reduced colony density of SK-N-AS cells (n = 8, $F(5, 42) = 8.063$, $p < 0.0001$; multiple comparisons: *$p < 0.05$ and ***$p < 0.001$ compared with control, one-way ANOVA with *post hoc* Dunnett's multiple comparisons test). Note that TG6-129 did not decrease the neurosphere size or colony formation in EP2-deleted SK-N-AS cell lines. Data are presented as mean + SEM.

(E) WT or EP2-deleted human NB cells SK-N-AS were inoculated (3×10^6 cells per site) into athymic nude mice (female, 6 weeks). After solid tumors became visible, tumor volumes were measured daily using the formula: $V = (width)^2 \times (length) \times 0.5$, and compared (n = 6–12, $F(2, 21) = 4.695$, $p = 0.0206$; multiple comparisons: $p = 0.0488$ and 0.0399 for EP2 KO1 and KO2 compared with WT cell line, respectively, two-way ANOVA and *post hoc* Dunnett's multiple comparisons test). Data are presented as mean ± SEM.

(F) Tumors formed by WT, KO1, and KO2 cell lines were harvested and displayed for comparisons.

(G) The SK-N-AS xenografts formed by EP2 KO1 cells and KO2 cells did not differ in volume or weight, so they were combined for weight comparisons between WT and EP2 KO groups (n = 12, $p = 0.0121$, t test). Data are presented as mean + SEM.

(H) EP2 expression was detected in tumors formed by WT cells, but not in tumors of EP2 KO cells, by immunostaining for EP2 (green fluorescence). Note that nuclei within each tumor were counterstained with DAPI (blue fluorescence). Scale bar, 50 μm.
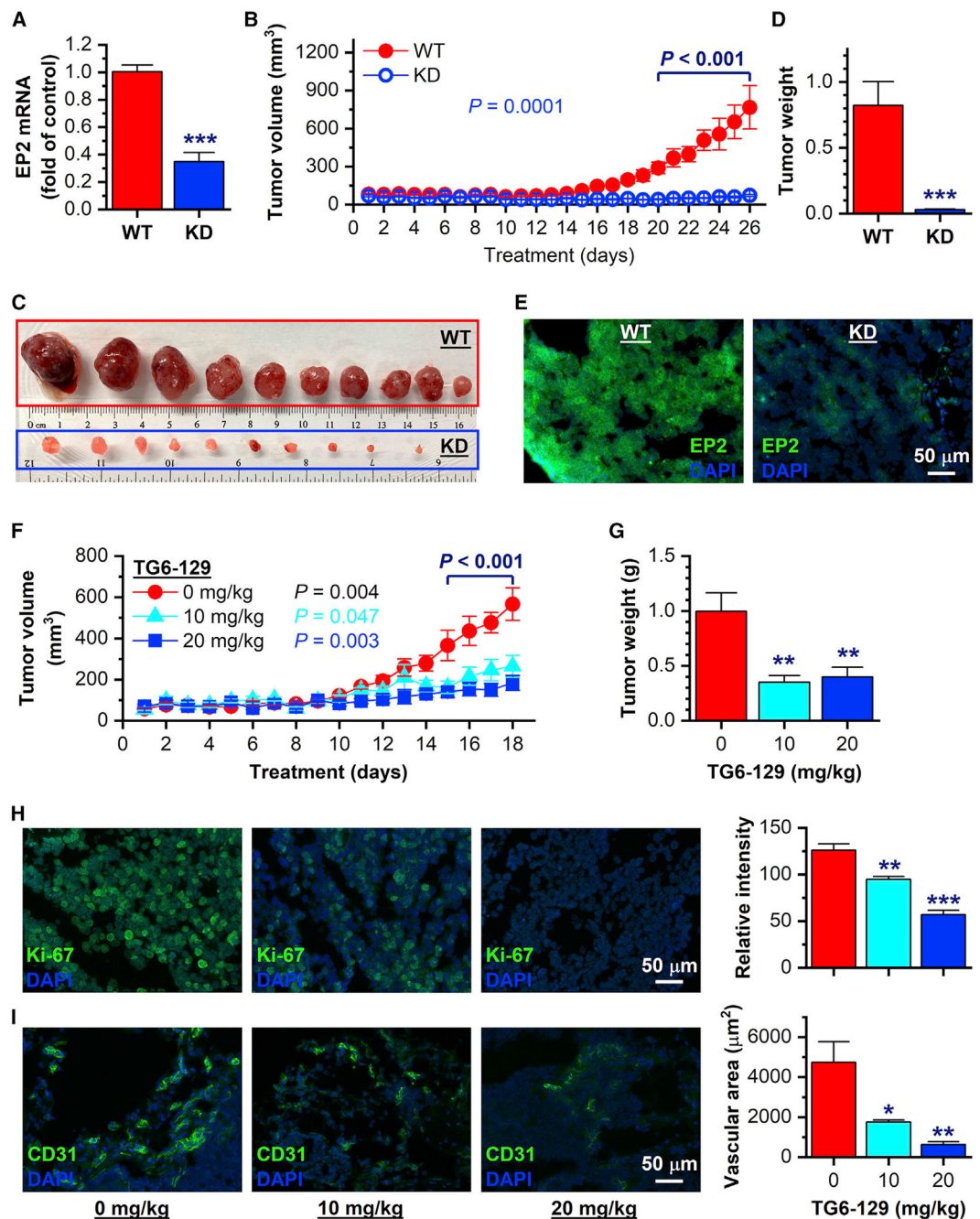
Figure 5. Conditional knockdown (KD) or pharmacological inhibition of EP2 impairs 11q-deleted NB growth

(A) Human 11q-deleted SK-N-AS cells with conditional KD of EP2 were generated using Tet-inducible lentiviral shRNA. EP2 shRNA was induced by doxycycline (0.5 μg/mL), and the efficacy of KD was validated by qPCR to measure EP2 mRNA levels. EP2 expression was significantly decreased in EP2 KD cells by >65% when compared with WT cells (n = 4; ***p < 0.001, t test). Data are presented as mean + SEM.

(B) WT or EP2 KD SK-N-AS cells were inoculated (5×10^6 cells per site) into athymic nude mice (female, 6 weeks). After solid tumors were well established, animals were treated

with doxycycline (50 mg/kg i.p.) daily to deplete EP2 in tumor cells. Tumor volumes were measured and compared (n = 10, $F(1, 18) = 23.9$, p = 0.0001; multiple comparisons: ***p < 0.001, two-way ANOVA and *post hoc* Dunnett's multiple comparisons test). Data are presented as mean ± SEM.

(C) Tumors formed by WT and EP2 KD cell lines were collected and displayed.

(D) Xenografts formed by WT and EP2 KD cells were weighed and compared (n = 10; ***p < 0.001, t test). Data are presented as mean + SEM.

(E) EP2 expression in WT and EP2 KD tumor tissues was examined by immunostaining (green fluorescence). Scale bar, 50 μm.

(F) SK-N-AS cells were inoculated into athymic nude mice (female, 6 weeks) with two injection sites per animal: 5×10^6 cells and 10×10^6 cells on each flank side. After solid tumors were developed, vehicle or selective EP2 antagonist TG6-129 (10 or 20 mg/kg i.p.) was administered daily for 18 consecutive days. Tumor growth was monitored by measuring tumor volume daily. The SK-N-AS xenograft tumors formed by 5×10^6 cells and 10×10^6 cells did not differ in growth or size, so they were combined for comparisons between treatment groups (n = 8–10, $F(2, 23) = 7.043$, p = 0.004; multiple comparisons: p = 0.047 and 0.003 for 10 mg/kg treatment and 20 mg/kg treatment compared with control, respectively, two-way ANOVA and *post hoc* Dunnett's multiple comparisons test). Data are presented as mean ± SEM.

(G) Tumors were harvested after 18-day treatment for comparisons. All tumors were weighed and compared between treatment groups (n = 8–10, $F(2, 23) = 8.645$, p = 0.002; multiple comparisons: p = 0.003 for 10 mg/kg treatment and p = 0.005 for 20 mg/kg treatment compared with control, one-way ANOVA with *post hoc* Dunnett's multiple comparisons test). Data are presented as mean + SEM.

(H) Immunostaining for Ki-67 (green fluorescence) was performed to identify proliferating cells in subcutaneous tumor tissues. Ki-67 expression levels were measured via quantifying the fluorescence intensity using ImageJ software and compared among groups (n = 4–5, $F(2, 10) = 39.87$, p < 0.001; multiple comparisons: p = 0.004 for 10 mg/kg treatment and p < 0.001 for 20 mg/kg treatment compared with control, one-way ANOVA with *post hoc* Dunnett's multiple comparisons test). Data are presented as mean + SEM. Scale bar, 50 μm.

(I) Immunostaining for CD31 (PECAM-1, green fluorescence) was utilized to indicate the microvessel density in subcutaneous tumors. CD31 levels were assessed via quantifying the fluorescence intensity and compared (n = 4–5, $F(2, 10) = 9.248$, p = 0.005; multiple comparisons: p = 0.025 for 10 mg/kg treatment and p < 0.004 for 20 mg/kg treatment compared with control, one-way ANOVA with *post hoc* Dunnett's multiple comparisons test). Note that nuclei within each tumor were counterstained with DAPI (blue fluorescence). Data are presented as mean + SEM. Scale bar, 50 μm.
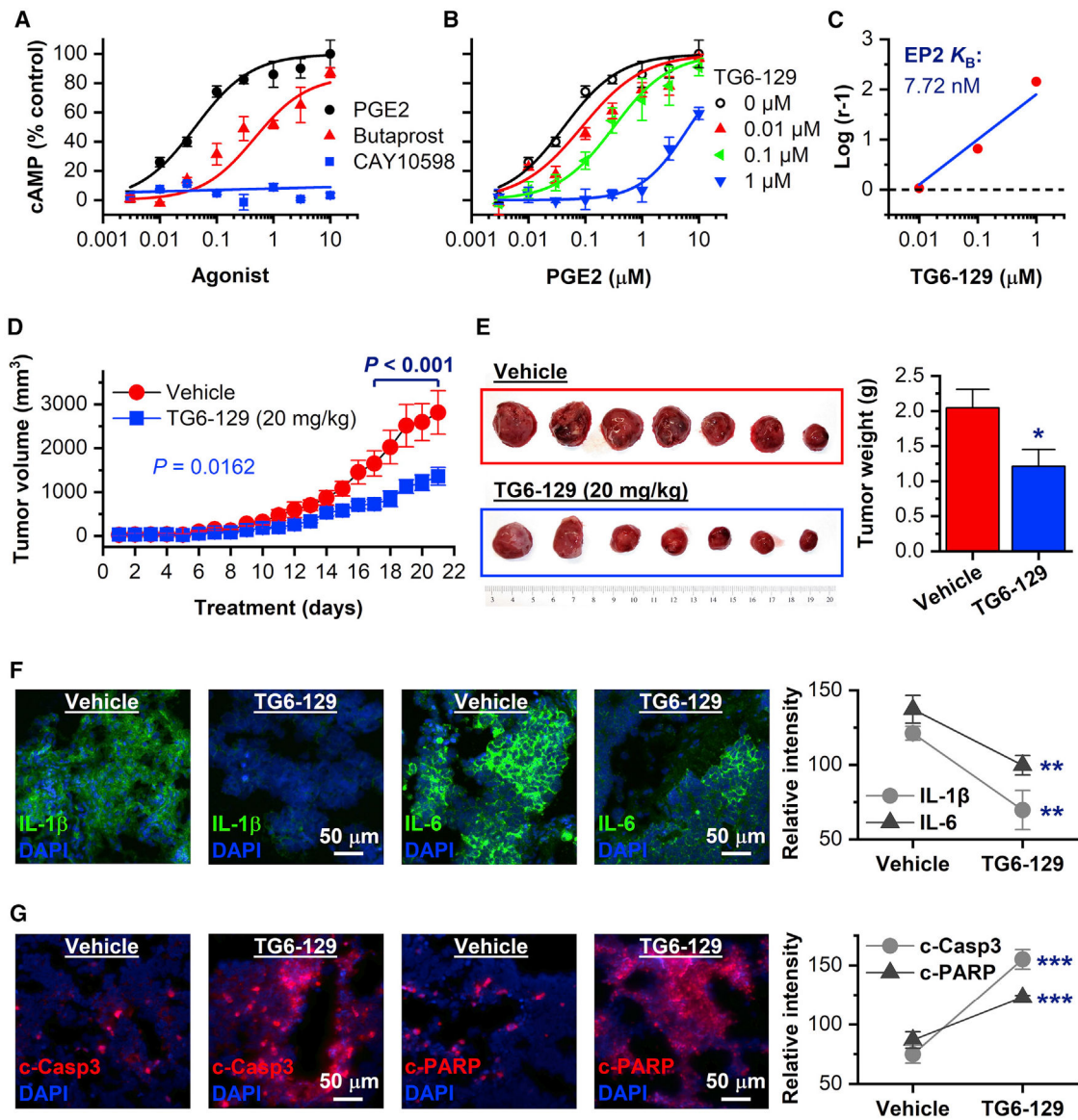
Figure 6. EP2 inhibition suppresses *MYCN*-amplified NB, reduces inflammation, and promotes apoptosis

(A) PGE$_2$ and selective EP2 agonist butaprost, but not EP4 agonist CAY10598, induced cAMP in human *MYCN*-amplified cell line BE(2)-C in a concentration-dependent manner (n = 4). The calculated PGE$_2$ EC$_{50}$ was 0.04 μM and butaprost EC$_{50}$ was 0.47 μM. Data are presented as mean ± SEM.

(B) EP2 antagonist TG6-129 inhibited PGE$_2$-stimulated cAMP in BE(2)-C cells in a concentration-dependent manner (n = 4). PGE$_2$ EC$_{50}$ values: 0.04 μM for control; 0.09, 0.32, and 6.07 μM for 0.01, 0.1, and 1 μM TG6-129. Data are presented as mean ± SEM.

(C) TG6-129 inhibited EP2 via a competitive mechanism in BE(2)-C cells, revealed by Schild regression analysis (K_B = 7.72 nM).
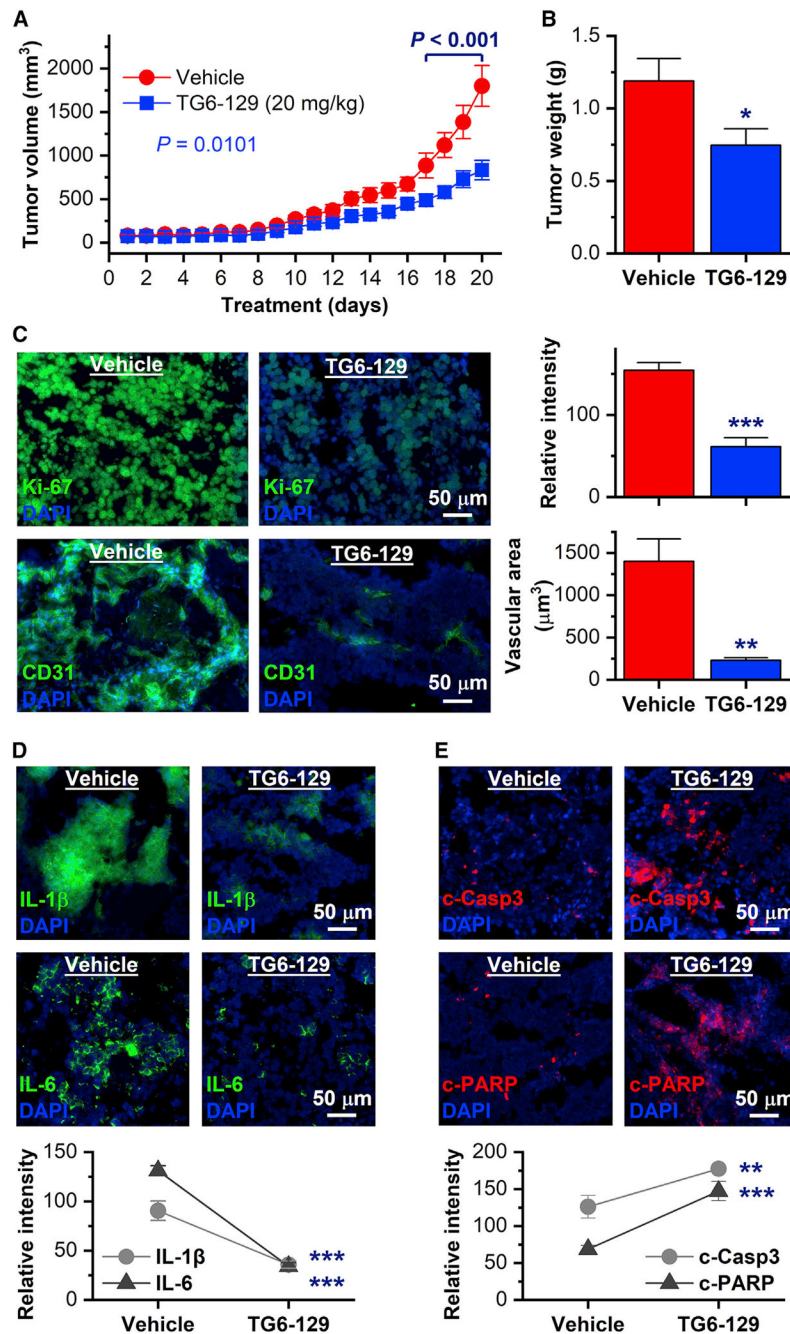
(D) BE(2)-C cells (3×10^6 cells per site) were inoculated into athymic nude mice (female, 6 weeks). After solid tumors were developed, vehicle or selective EP2 antagonist TG6-129 (20 mg/kg i.p.) was administered daily for 3 weeks. Tumor growth was monitored by

measuring tumor volume daily and compared (n = 7, $F(1, 12)$ = 7.81, p = 0.0162; multiple comparisons: ***p < 0.001, two-way ANOVA and *post hoc* Dunnett's multiple comparisons test). Data are presented as mean ± SEM.

(E) Tumors were displayed, weighed, and compared between treatment groups (n = 7; p = 0.0376, t test). Data are presented as mean + SEM.

(F) Immunostaining for cytokines IL-1β and IL-6 (green fluorescence) was utilized to indicate the inflammation in subcutaneous tumors. Cytokine levels were assessed via quantifying the fluorescence intensity and compared (n = 7, p = 0.003 and p = 0.0057 for IL-1β and IL-6, respectively, t test). Data are presented as mean ± SEM. Scale bar, 50 μm.

(G) Immunostaining for cleaved caspase-3 (c-Casp3) and cleaved PARP (c-PARP) (red fluorescence) was performed to indicate apoptosis in subcutaneous tumors from mice treated by vehicle and TG6-129. Protein levels of c-Casp3 and c-PARP were assessed via quantifying the fluorescence intensity and compared (n = 5, p < 0.001 for both c-Casp3 and c-PARP, t test). Note that nuclei within each tumor were counterstained with DAPI (blue fluorescence). Data are presented as mean ± SEM. Scale bar, 50 μm.

Figure 7. Pharmacological inhibition of EP2 receptor suppresses syngeneic NB in immunocompetent hosts

(A) Mouse NXS2 NB cells (2×10^6 cells per site) were inoculated into immunocompetent A/J mice (female, 6 weeks). After solid tumors were detected, vehicle or TG6-129 (20 mg/kg i.p.) was administered to mice daily for 3 weeks. Tumor growth was monitored by measuring tumor volume daily and compared (n = 10, $F(1, 18) = 8.257$, p = 0.0101; multiple comparisons: ***p < 0.001, two-way ANOVA and *post hoc* Dunnett's multiple comparisons test). Data are presented as mean ± SEM.

(B) Tumors were harvested and weighed for comparison between treatment groups (n = 10; *p < 0.05, t test). Data are presented as mean + SEM.

(C) Immunostaining for Ki-67 (green fluorescence) was performed to identify proliferating cells in tumors treated by vehicle or TG6-129 (n = 10; ***p < 0.001, t test). Immunostaining for CD31 (PECAM-1, green fluorescence) was utilized to indicate angiogenesis (n = 10; **p < 0.01, t test). Data are presented as mean + SEM. Scale bar, 50 μm.

(D) Immunostaining for cytokines IL-1β and IL-6 (green fluorescence) was employed to indicate the inflammation in allograft tumors. Cytokine levels were assessed via quantifying the fluorescence intensity and compared (n = 5; ***p < 0.001, t test). Data are presented as mean ± SEM. Scale bar, 50 μm.

(E) Immunostaining for c-Casp3 and c-PARP (red fluorescence) was performed to assess apoptosis in allograft tumors from mice treated by vehicle and TG6-129. Protein levels of c-Casp3 and c-PARP were measured via quantifying the fluorescence intensity and compared (n = 5; **p < 0.01 for c-Casp3 and ***p < 0.001 for c-PARP, t test). Note that nuclei within each tumor were counterstained with DAPI (blue fluorescence). Data are presented as mean ± SEM. Scale bar, 50 μm.

KEY RESOURCES TABLE

REAGENT or RESOURCE	SOURCE	IDENTIFIER
Antibodies		
Rabbit anti-Ki-67	Biocare Medical	Cat# CRM325B; RRID: AB_2721189
Rat anti-CD31(PECAM-1)	eBioscience	Cat# 14-0311-82; RRID: AB_467201
Rabbit anti-EP2 receptor	Cayman Chemical	Cat# 101750; RRID: AB_10078697
Mouse anti-IL-1β	Cell Signaling Technology	Cat# 12242S; RRID: AB_2715503
Goat anti-IL-6	Santa Cruz Biotechnology	Cat# sc-1265; RRID: AB_2127470
Rabbit anti-cleaved caspase-3	Cell Signaling Technology	Cat# 9664T; RRID: AB_2070042
Rabbit anti-cleaved PARP	Cell Signaling Technology	Cat# 5625S; RRID: AB_10699459
Goat anti-rabbit IgG, secondary, Alexa Fluor 488	Invitrogen	Cat# A-11034; RRID: AB_2576217
Goat anti-rabbit IgG, secondary, Alexa Fluor 546	Invitrogen	Cat# A-11035; RRID: AB_2534093
Goat anti-mouse IgG, secondary, Alexa Fluor 488	Invitrogen	Cat# A-11001; RRID: AB_2534069
Goat anti-rat IgG, secondary, Alexa Fluor 488	Invitrogen	Cat# A-11006; RRID: AB_2534074
Bacterial and virus strains		
DH5α competent cells	Thermo Scientific	Cat# 18265017
Chemicals, peptides, and recombinant proteins		
PGE_2	Cayman Chemical	Cat# 14010; CAS# 363-24-6
Butaprost	Cayman Chemical	Cat# 13740; CAS# 69685-22-9
CAY10598	Cayman Chemical	Cat# 13281; CAS# 346673-06-1
PF-04418948	Cayman Chemical	Cat# 15016; CAS# 1078166-57-0
GW627368X	Cayman Chemical	Cat# 10009162; CAS# 439288-66-1
Rolipram	Sigma-Aldrich	Cat# R6520; CAS# 61413-54-5
Forskolin	Sigma-Aldrich	Cat# F6886; CAS# 66575-29-9
TG6-129	This study	PubChem CID 1987175
TG4-155	This study	PubChem CID 5886965
TG6-10-1	This study	PubChem CID 71499384
SID26671393	ChemBridge	PubChem CID 1830592
Iscove's Modified Dulbecco's Medium	Gibco	Cat# 12440061
L-Glutamine (200 mM)	Gibco	Cat# A2916801
Insulin-Transferrin-Selenium (ITS)	Gibco	Cat# 41400045
Lipofectamine 2000	Invitrogen	Cat# 11668019
FastDigest BsmBI (Esp3I)	Thermo Scientific	Cat# FD0454
T4 DNA ligase	New England Biolabs	Cat# M0202S
T4 Polynucleotide Kinase	New England Biolabs	Cat# M0201S
Polybrene	Sigma-Aldrich	Cat# TR-1003-G
Puromycin Dihydrochloride	Gibco	Cat# A1113803
Doxycycline hyclate, 98%	Thermo Scientific	Cat# AC446060050
PEG 400	Sigma-Aldrich	Cat# 91893; CAS# 25322-68-3
Critical commercial assays		
cAMP Gs dynamic kit	Cisbio Bioassays	Cat# 62AM4PEC

REAGENT or RESOURCE	SOURCE	IDENTIFIER
PureLink RNA Mini Kit	Invitrogen	Cat# 12183018A
SuperScript III First-Strand Synthesis System	Invitrogen	Cat# 18080051
SYBR Green Supermix	Bio-Rad Laboratories	Cat# 1725271
Deposited data		
Neuroblastoma patient datasets: SEQC, Kocak, Versteeg, and NRC	The R2 Genomics Platform	http://r2.amc.nl
Experimental models: Cell lines		
Human SK-N-AS	ATCC	Cat# CRL-2137; RRID: CVCL_1700
Human SK-N-AS (EP2 KO1 and KO2)	This study	N/A
Human SK-N-AS (EP2 KD)	This study	N/A
Human SK-N-SH	ATCC	Cat# HTB-11; RRID: CVCL_0531
Human SH-SY5Y	ATCC	Cat# CRL-2266; RRID: CVCL_0019
Human SK-N-BE(2)	ATCC	Cat# CRL-2271; RRID: CVCL_0528
Human BE(2)-C	ATCC	Cat# CRL-2268; RRID: CVCL_0529
Human IMR-32	ATCC	Cat# CCL-127; RRID: CVCL_0346
Mouse Neuro-2a	ATCC	Cat# CRL-131; RRID: CVCL_0470
Human Hs68	ATCC	Cat# CRL-1635; RRID: CVCL_0839
Human 293T	ATCC	Cat# CRL-3216; RRID: CVCL_0063
Human CHLA-90	Childhood Cancer Repository	RRID: CVCL_6610
Human CHLA-136	Childhood Cancer Repository	RRID: CVCL_6590
Human NB-EBc1	Childhood Cancer Repository	RRID: CVCL_e218
Human NB-1691	Childhood Cancer Repository	RRID: CVCL_5628
Human SiMa	DSMZ-German Collection of Microorganisms and Cell Cultures	Cat# ACC 164; RRID: CVCL_1695
Mouse NXS2	Scripps Research Institute	N/A
Experimental models: Organisms/strains		
Athymic nude mice, Crl:NU(NCr)-*Foxn1*[nu]	Charles River Laboratories	Strain Code# 490
Athymic nude mice, Hsd:Athymic nude-*Foxn1*[nu]	Envigo	Order Code# 069
A/J mice	Jackson Laboratory	Strain# 000646; RRID: IMSR_JAX:000646
Oligonucleotides		
CRISPR/Cas9, human EP2 KO1 forward (5′-3′), CACCGCGTACGAAGCCAGTACCACT	This study	N/A
CRISPR/Cas9, human EP2 KO1 reverse (5′-3′), AAACAGTGGTACTGGCTTCGTACGC	This study	N/A
CRISPR/Cas9, human EP2 KO2 forward (5′-3′), CACCGGGTCATGGCGAAAGCGAAGT	This study	N/A
CRISPR/Cas9, human KO2 reverse (5′-3′), AAACACTTCGCTTTCGCCATGACCC	This study	N/A
Primer for qPCR, human EP2 forward (5′-3′), TTGGGTCTTTGCCATCCTTAG	This study	N/A
Primer for qPCR, human EP2 reverse (5′-3′), AGGAAGTTTGTGTTGCATCTTG	This study	N/A

REAGENT or RESOURCE	SOURCE	IDENTIFIER
Primer for qPCR, human GAPDH forward (5′-3′), GTCAAGGCTGAGAACGGGAA	This study	N/A
Primer for qPCR, human GAPDH reverse (5′-3′), AAATGAGCCCCAGCCTTCTC	This study	N/A
Recombinant DNA		
Lentiviral envelope expressing plasmid pMD2.G	Addgene	Cat# 12259
Lentiviral packaging plasmid psPAX2	Addgene	Cat# 12260
Lentiviral vector lentiCRISPR v2	Addgene	Cat# 52961
pTRIPZ inducible lentiviral shRNA targeting human EP2	Horizon Discovery	Clone ID# V2THS_131491
Software and algorithms		
OriginPro 2019	OriginLab	https://www.originlab.com/
GraphPad Prism 8	GraphPad Software	https://www.graphpad.com/scientific/software/prism
ImageJ	NIH	https://imagej.nih.gov/ij/
BioRad CFX Maestro	Bio-Rad Laboratories	https://www.bio-rad.com/en-us/sku/12013758-cfx-maestro-software
Gen5	BioTek Instruments	https://www.biotek.com/products/software-robotics-software/gen5-microplate-reader-and-imager-software/
Other		
Fluorescence microscope BZ-X800	KEYENCE	N/A
NanoDrop One microvolume spectrophotometer	Thermo Scientific	N/A
Bio-Rad C1000 Touch Thermal Cycler	Bio-Rad Laboratories	N/A
Bio-Rad T100 Thermal Cycler	Bio-Rad Laboratories	N/A
Synergy H1 Hybrid Multi-Mode Reader	BioTek Instruments	N/A
2104 Envision Multilabel Plate Reader	PerkinElmer	N/A
HM525 NX Cryostat	Thermo Scientific	N/A